Molecular Therapy
Original Article

Dominant-Negative TGF-β Receptor Enhances PSMA-Targeted Human CAR T Cell Proliferation And Augments Prostate Cancer Eradication

Christopher C. Kloss,[1,4] Jihyun Lee,[1,5] Aaron Zhang,[1] Fang Chen,[1] Jan Joseph Melenhorst,[1,2,3] Simon F. Lacey,[1] Marcela V. Maus,[1,6] Joseph A. Fraietta,[1,2,3] Yangbing Zhao,[1,2] and Carl H. June[1,2,3,4]

[1]Center for Cellular Immunotherapies, Perelman School of Medicine, University of Pennsylvania, Philadelphia, PA 19104-5156, USA; [2]Department of Pathology and Laboratory Medicine, Perelman School of Medicine, University of Pennsylvania, Philadelphia, PA 19104-5156, USA; [3]Parker Institute for Cancer at the University of Pennsylvania, Philadelphia, PA 19104-5156, USA; [4]Smilow Center for Translational Research, 3400 Civic Center Blvd., Philadelphia, PA 19104-5156, USA

Cancer has an impressive ability to evolve multiple processes to evade therapies. While immunotherapies and vaccines have shown great promise, particularly in certain solid tumors such as prostate cancer, they have been met with resistance from tumors that use a multitude of mechanisms of immunosuppression to limit effectiveness. Prostate cancer, in particular, secretes transforming growth factor β (TGF-β) as a means to inhibit immunity while allowing for cancer progression. Blocking TGF-β signaling in T cells increases their ability to infiltrate, proliferate, and mediate antitumor responses in prostate cancer models. We tested whether the potency of chimeric antigen receptor (CAR) T cells directed to prostate-specific membrane antigen (PSMA) could be enhanced by the co-expression of a dominant-negative TGF-βRII (dnTGF-βRII). Upon expression of the dominant-negative TGF-βRII in CAR T cells, we observed increased proliferation of these lymphocytes, enhanced cytokine secretion, resistance to exhaustion, long-term *in vivo* persistence, and the induction of tumor eradication in aggressive human prostate cancer mouse models. Based on our observations, we initiated a phase I clinical trial to assess these CAR T cells as a novel approach for patients with relapsed and refractory metastatic prostate cancer (ClinicalTrials.gov: NCT03089203).

INTRODUCTION

Prostate cancer is the most common and second most deadly cancer for men. Upon metastasis to bone, the disease usually becomes refractory to therapy and often results in death within 3–5 years.[1] Metastatic prostate cancer is minimally responsive to checkpoint blockade of PD-1 and CTLA-4.[2]

The recent medical breakthroughs of cancer immunotherapy have demonstrated the power that harnessing the immune system can have to eliminate cancer cells.[3] Most of these therapies rely on the triggering of immune responses upon administering monoclonal antibodies that block various immunosuppressive signals.[4,5] However, relying on endogenous responses makes it difficult to achieve high therapeutic efficacy while avoiding toxic autoimmune side effects.[6]

For more precise therapy, T cells can be engineered with chimeric antigen receptor (CAR) constructs to recognize and exert cytotoxic effects on cells expressing specific antigens.[7,8] A challenge to the success of these therapies is the immunosuppressive microenvironment that re-directed T cells encounter upon infiltration into the tumor bed.[9,10]

To achieve therapeutic success within solid tumors, CAR T cells need to overcome immunosuppressive signals. One approach is to block immunosuppressive pathways such as PD-1 and/or CTLA-4 in combination with CAR T cells to achieve an enhanced response.[11,12] Many cancers, particularly prostate cancer, are known to secrete transforming growth factor β (TGF-β), creating an immunosuppressive milieu. TGF-β is known to induce or promote metastasis and neoangiogenesis and to potently suppress the immune system.[13–15] Studies in the 1990s demonstrated that TGF-β signaling can be blocked by using a dominant-negative TGFBRII (dnTGF-βRII), which is truncated and lacks the intracellular domain necessary for downstream signaling.[16,17] Expression of the dnTGF-βRII enhances antitumor immunity and can lead to autoimmunity.[18,19] Furthermore, transgenic mice expressing dnTGF-βRII develop a lymphoproliferative disorder.[20] Two studies demonstrated enhanced T cell infiltration into tumors with potent antitumor responses in the transgenic adenocarcinoma mouse prostate (TRAMP) mouse model of prostate cancer when utilizing this receptor.[21,22] A clinical trial (ClinicalTrials.gov: NCT00368082) testing the safety and efficacy of the dnTGF-βRII receptor in Epstein-Barr virus (EBV)-specific T cells for lymphoma was recently reported.[23,24]

Received 13 January 2018; accepted 4 May 2018;
https://doi.org/10.1016/j.ymthe.2018.05.003.

[5]Present address: LG Chem, Ltd., Seoul, South Korea

[6]Present address: Massachusetts General Hospital, Boston, MA 02114, USA

Correspondence: Christopher C. Kloss, Smilow Center for Translational Research, 3400 Civic Center Blvd., Philadelphia, PA 19104-5156, USA.
E-mail: klosschr@pennmedicine.upenn.edu

Correspondence: Carl H. June, Smilow Center for Translational Research, 3400 Civic Center Blvd., Philadelphia, PA 19104-5156, USA.
E-mail: cjune@upenn.edu

Glutamate carboxypeptidase II or prostate-specific membrane antigen (PSMA) is a type II membrane glycoprotein that has been studied within the prostate cancer field for three decades as a tumor-associated antigen for prostate cancer. There is low-level expression in some normal tissues (e.g., astrocytes, neurons, kidney epithelium, and salivary gland). Many methodologies use PSMA either for positron emission tomography (PET) imaging or for antibody-targeted therapies.[25] In addition, a trial has been open since 2010 using anti-PSMA CAR T cells employing a CD28 costimulatory and CD3ζ activation domain with reported limited persistence of the CAR T cells and no observed responses (ClinicalTrials.gov: NCT01140373), indicating a need for a more potent PSMA-specific CAR T cell.

We reasoned that co-expressing the dnTGF-βRII with a PSMA-specific CAR in T cells would result in enhanced infiltration, proliferation, persistence, and efficacy when treating prostate cancer. We characterized the mechanisms underlying the potency-enhancing effects of TGF-β blockade in anti-PSMA Pbbz CAR T cells.

RESULTS

The design of the CARs used in these studies is described in the Materials and Methods. All CARs used the 4-1BB costimulatory and CD3ζ-signaling domains that are in tisagenlecleucel, the CAR recently approved by the U.S. Food and Drug Administration for leukemia. Employing lentiviral vectors, we routinely obtain 30%–60% transduction efficiencies of primary human T cells using an MOI of 1 to 2. Mock-transduced cells were included to control for allogeneic effects. A mismatched CAR was included that targets CD19 (tisagenlecleucel, 19BBZ) to control for antigen-independent effects of the CAR components. In the case of the anti-PSMA CAR (Pbbz), the scFv was derived from the mouse J591 monoclonal antibody that had been previously humanized.[26]

Utilizing a T2A element, we obtained efficient co-expression of the dnTGF-βRII with the Pbbz CAR (dnTGF-βRII-T2A-Pbbz (Figure 1A). This dnTGF-βRII functions to block TGF-β signaling, which was demonstrated by differential SMAD2/3 phosphorylation in CAR-positive and CAR-negative cells upon stimulation with human TGF-β (Figure 1B). The Pbbz CAR functioned to induce specific lysis of human prostate cancer cells only when they expressed PSMA (Figure 1C). The PC3 prostate cancer cell line was verified to secrete high levels of latent TGF-β (Figure 1D). When these PC3-PSMA$^+$ tumor cells were used for long-term co-culture experiments with Pbbz CAR T cells, the CAR T cells co-expressing the dnTGF-βRII had a much higher population doubling observed, with ∼15-fold higher proliferation over 42 days co-culture and repetitive stimulation with PSMA-expressing tumor cells (Figure 1E). This enhanced proliferation was antigen dependent, because it was not observed in cultures of CAR T cells with or without tumor cells that did not express PSMA (Figure 1E, top panels).

Intrigued by the ability of dnTGF-βRII-T2A-Pbbz CAR T cells to proliferate more efficiently than Pbbz alone in the presence of tumor cells that secrete TGF-β, we next interrogated these *in vitro* co-cultures more closely. At days 0, 7, 14, 21, and 28, we harvested the T cells and supernatant for analyses. The CD8+ T cell percentage declined from the routinely obtained 30% at baseline to 7.8% in Pbbz and 5.0% in dnTGF-βRII-T2A-Pbbz by day 28. There was a modest increase from 1.56% to 3.55% of CD4+ CAR T cells that expressed CD127. We found that there was a statistically higher percentage of central memory CD8$^+$ T cells with a significant loss of FoxP3 staining from 38% in Pbbz to 25% in dnTGF-βRII-T2A-Pbbz (Figures 2A and 2B). From cytokine analysis, we determined that T_H2 cytokines (i.e., interleukin-4 [IL-4], IL-5, and IL-13) were differentially secreted at higher amounts in dnTGF-βRII-T2A-Pbbz than in Pbbz (Figure 2C). IL-2 secretion by the PSMA Pbbz CAR T cells was similar with or without dnTGF-βRII. In addition, the innate immune cell-recruiting cytokines IP-10, MIP1-α, MIP1-β, and RANTES were elevated in the dnTGF-βRII-T2A-Pbbz group compared to the Pbbz group.

By harvesting total mRNA from these T cells at spaced time intervals after the initiation of culture, we performed longitudinal whole-transcriptome and microRNA microarray analysis. Interestingly, at 7 days of co-culture with PC3-PSMA, these dnTGF-βRII-T2A-Pbbz T cells only had 16 differentially expressed (>2- or <−2-fold change) genes or microRNAs (Table S1). Most of these were either unannotated genes or microRNAs. After 14 days, there were 51 differentially expressed genes or microRNAs. Finally, after 21 days there were 343 differentially expressed genes or microRNAs. Confirmed by cytokine analysis, IL-4, IL-5, and IL-13 were among the highest differentially expressed genes (DEGs) in the dnTGF-βRII-T2A-Pbbz group. Other highly DEGs of interest included EOMES, IFNG, PTGDR2, EPAS1, EGR1, and ARG2 (Figure S1; Table S1).

A protein-protein interaction (PPI) network was constructed using the DEGs on days 14 and 21 of co-culture with the PC3-PSMA tumor cells (Figure 3). The PPI was constructed using STRING.[27] On day 14, the analysis shown in Figure 3A indicates that more inter-protein interactions were found than expected by random interaction ($p < 1.3 \times 10^{-14}$). There were 3 clusters of proteins preferentially interacting in dnTGF-βRII-T2A-Pbbz PSMA CAR T cells on day 14. One cluster comprised cytokine-related proteins (IL-4, IL-5, SOCS1, IL-23R, PTGDR2, TLR7, etc.), another comprised transcription factors (FOS, FOSL2, EGR1, JUN, JUNB, and JUND), and the last, hypoxia-related factors (ARNT, EGLN3, and EPAS1). In contrast, on day 21 there were 2 main clusters of predicted functional or structural PPIs (Figure 3B): one comprised cell cycle-related proteins (CCNA1, CCNA2, CCNB1, CCNB2, CDK1, CDC20, CDC20B, CDC45, CKS, CKS1B, and TP73), and the other, cytokines and chemokines (leukemia inhibitory factor [LIF], interferon [IFN]-γ, IL-1A, IL-3RA, IL-4, IL-5, colony-stimulating factor 2 [CSF2], oncostatin M [OSM], IL-13, and CCL3).

The DEGs were then mapped to the Kyoto Encyclopedia of Genes and Genomes (KEGG) pathways, and their enrichment for specific pathways was investigated using STRING analysis. On day 21, there were 24 KEGG pathways identified, including cell signaling (cytokine

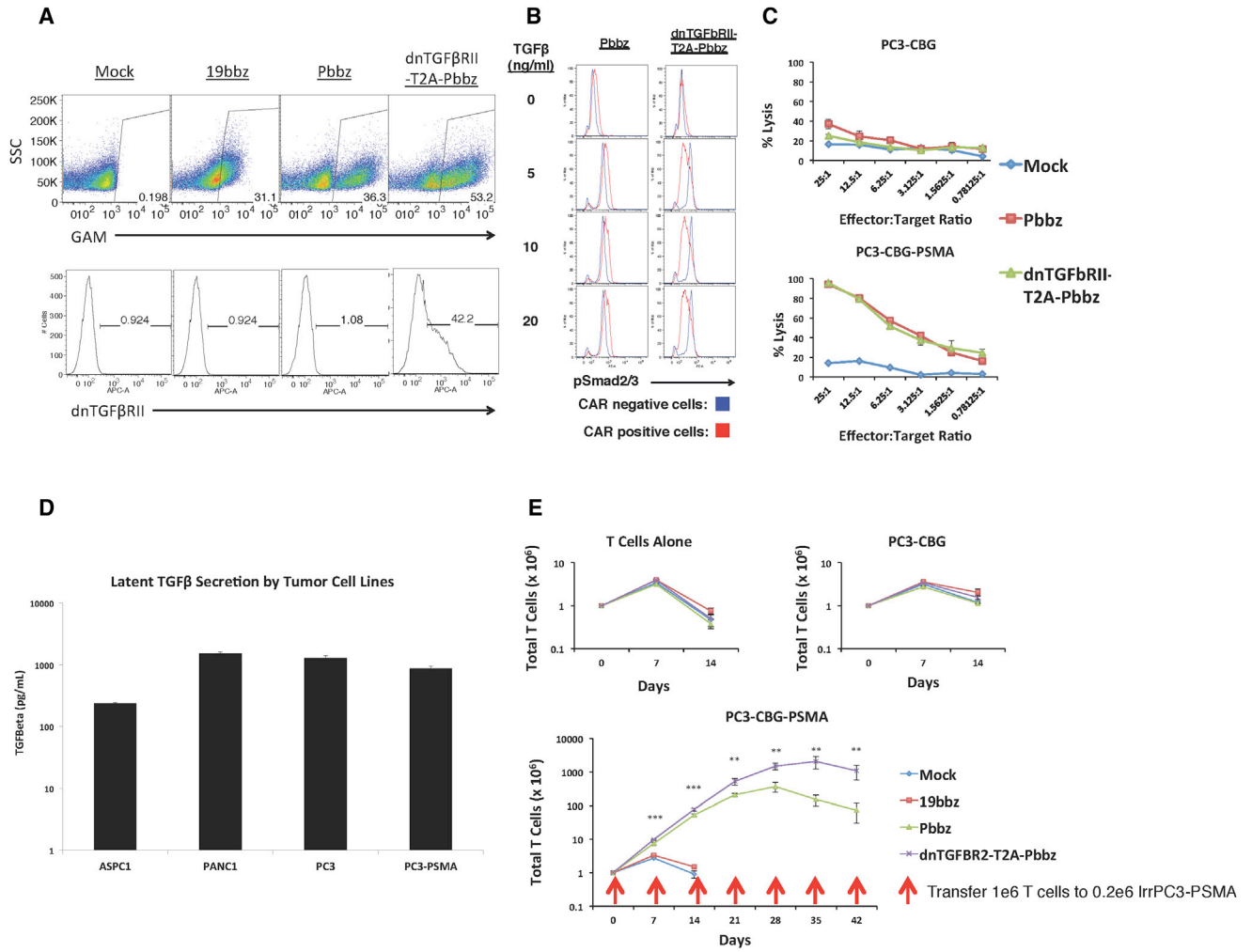

Figure 1. *In Vitro* Functionality of Pbbz CAR and dnTGF-βRII-T2A-Pbbz CAR

(A) Lentiviral transduction allows for efficient expression of 19bbz, Pbbz alone, or dnTGF-βRII-T2A-Pbbz in primary human T cells. (B) Expression of dnTGF-βRII prevents TGF-β signal induction through Smad2/3. (C) T cells expressing Pbbz specifically lyse PSMA$^+$ PC3 cells in 24-hr luciferase-based lysis assays. (D) ELISA determination of the secretion of the latent form of TGF-β by tumor lines. (E) Expression of dnTGF-βRII-T2A-Pbbz enhances antigen-specific proliferation of CAR T cells upon co-culture with PSMA$^+$ PC3 cells (y axis log10 scale). The error bars represent ± SD. **$p < 0.01$, and ***$p < 0.001$.

interactions, Jak-STAT, cell cycle, TCR signaling, and FcεR1 signaling) and autoimmunity (inflammatory bowel disease, rheumatoid arthritis, systemic lupus erythematosus, and type I diabetes) that were statistically significant associations (false discovery rates for all <0.005) (Table S2). The KEGG pathways identified on day 14 were similar. Finally, we also used the DEG to conduct gene ontology (GO) analysis. There were many biologic processes identified; the top 10 are shown in Table 1 and the entire list is shown in Table S3. The top GO terms identified on day 14 were biologic processes primarily related to effector immune responses, and on day 21, GO terms were related to cell cycle and cell division.

From these robust *in vitro* results, we postulated that the dnTGF-βRII-T2A-Pbbz CAR T cells had more sustained effector functions in the presence of tumor cells that express TGF-β than the CAR alone, based on the enhanced cytokine and cell cycle gene expression data. To test this hypothesis *in vivo*, we infused the PC3-PSMA human prostate cancer cells into NOD/SCID IL-2gamma (NSG) mice, allowing disseminated tumors to form in the mice within the lung, liver, bone, kidney, stomach, pancreas, head, and spinal cord. In this model, the mice died 4–6 weeks following tumor injection. The PC3-PSMA cells were engineered to express luciferase, allowing tumor burden to be easily quantified. After allowing these tumors to engraft and disseminate for 2 weeks, we infused 5×10^6 CAR T cells by tail vein (Figure 4A). It is evident from the tumor burden quantification that the dnTGF-βRII-T2A-Pbbz CAR T cells functioned significantly better than Pbbz CAR T cells alone and eradicated the tumor from these mice (Figure 4B). The images confirm that

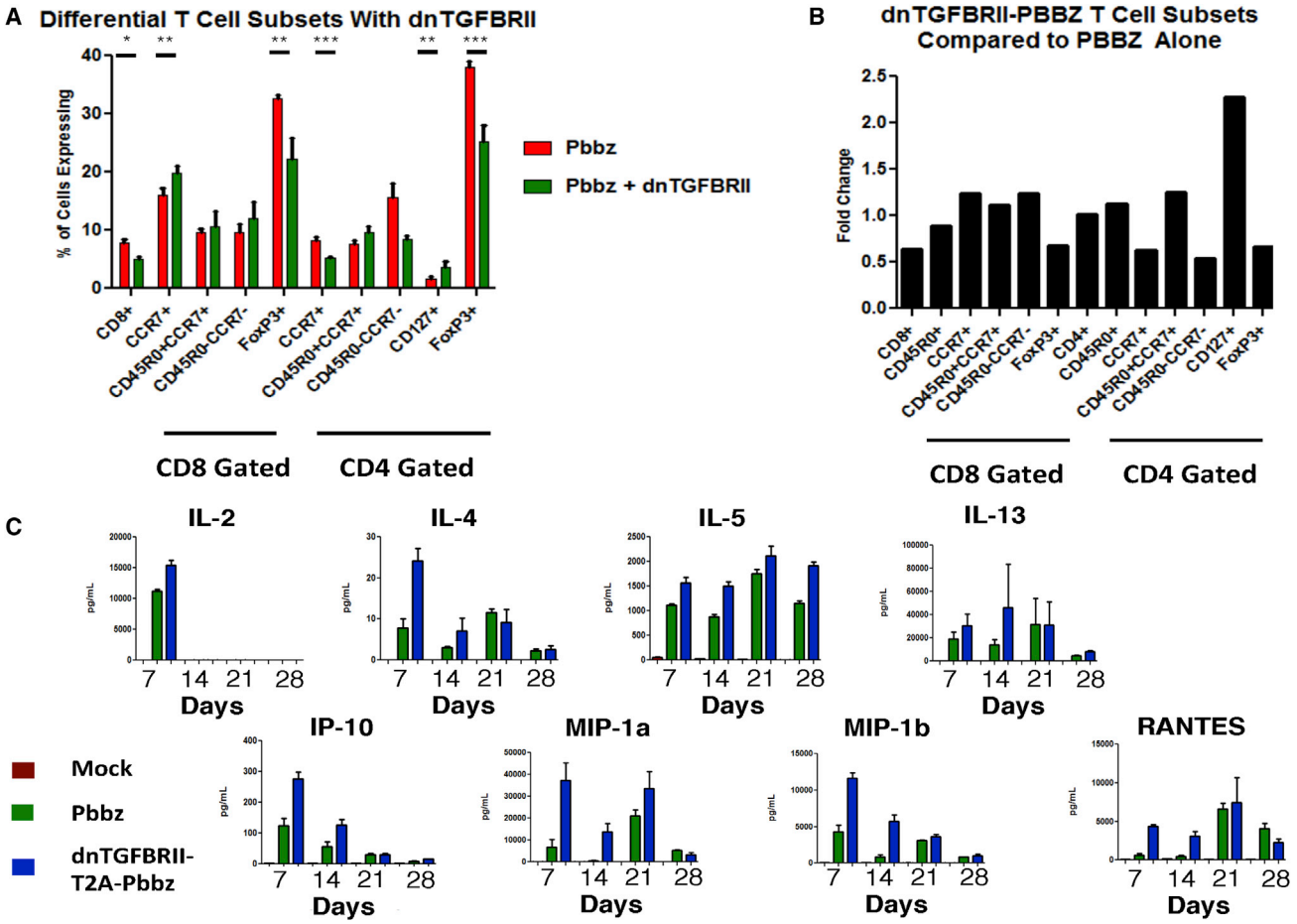

Figure 2. Flow Cytometric and Multiplex Cytokine Profiling of CAR T Cell Subsets from PC3-PSMA Co-culture

(A and B) T cells were analyzed with flow cytometry at day 21 post co-culture of Pbbz or dnTGF-βRII-T2A-Pbbz CAR T cells. (A) shows the differential percentage of various T cell subsets, which is further represented as fold change of T cell subsets found in the dnTGF-βRII-T2A-Pbbz versus Pbbz CAR T cells alone (B). (C) Luminex 30-Plex cytokine analysis was performed using T cell supernatants isolated at days 7, 14, 21, and 28 from Pbbz or dnTGF-βRII-T2A-Pbbz CAR T cells, as shown in Figure 1E. Pbbz-alone T cells, green bars; dnTGF-βRII-T2A-Pbbz T cells, blue bars. The error bars represent ± SD. *$p < 0.05$, **$p < 0.01$, and ***$p < 0.001$.

the dnTGF-βRII-T2A-Pbbz CAR T cells eliminated tumor in 4/4 mice, while the Pbbz T cells alone allowed for only 1/4 mice to achieve eradication (Figure 4C). In contrast all mice in the mock T cell group died from tumor progression 21–28 days after T cell injection. Interestingly, the levels of human T cells in the dnTGF-βRII-T2A-Pbbz group were 7 times higher in blood than the levels of Pbbz T cells, and 85% of these cells were $CD4^+$ CAR T cells (Figure 4D). In addition, the tumor-free mice in the dnTGF-βRII-T2A-Pbbz group began to have weight loss and developed signs of xenogeneic graft-versus-host disease (GVHD) (xGVHD), requiring euthanasia a month after CAR T cell infusion.

To further compare the CAR T cells *in vivo*, we used the PC3-PSMA NSG mouse metastatic prostate cancer model to perform a dose escalation trial of dnTGF-βRII-T2A-Pbbz PSMA CAR and Pbbz PSMA CAR T cells. At 2 weeks following tumor injection, doses of 0.5×10^6 and 2.5×10^6 CAR T cells were infused intravenously (i.v.) (Figure 5A); note that the dose used in the first experiment was 5×10^6 CAR T cells. In this experiment, we observed that the higher dose of dnTGF-βRII-T2A-Pbbz CAR T cells caused regression of tumor burden at day 14, while mice in the mock and CD19 CAR T cell control groups had progressive tumor burdens that required sacrifice according to predetermined endpoints of the protocol (Figure 5B). By day 42, 4/5 mice treated with PSMA dnTGF-βRII-T2A-Pbbz CAR T cells had tumor eradication (Figure 5D). In contrast, the mice given the lower dose of dnTGF-βRII-T2A-Pbbz CAR T cells had initial tumor control until day 21, followed by tumor relapse similar to the mice treated with PSMA Pbbz CAR T cells.

Intriguingly, the mice treated with the higher dose of dnTGF-βRII-T2A-Pbbz CAR T cells had a significant loss of body weight between days 28 and 35, but then they recovered to previous weight by day 42 following tumor elimination (Figure 5C). The mechanism of the reversible weight loss is not known, but it may be

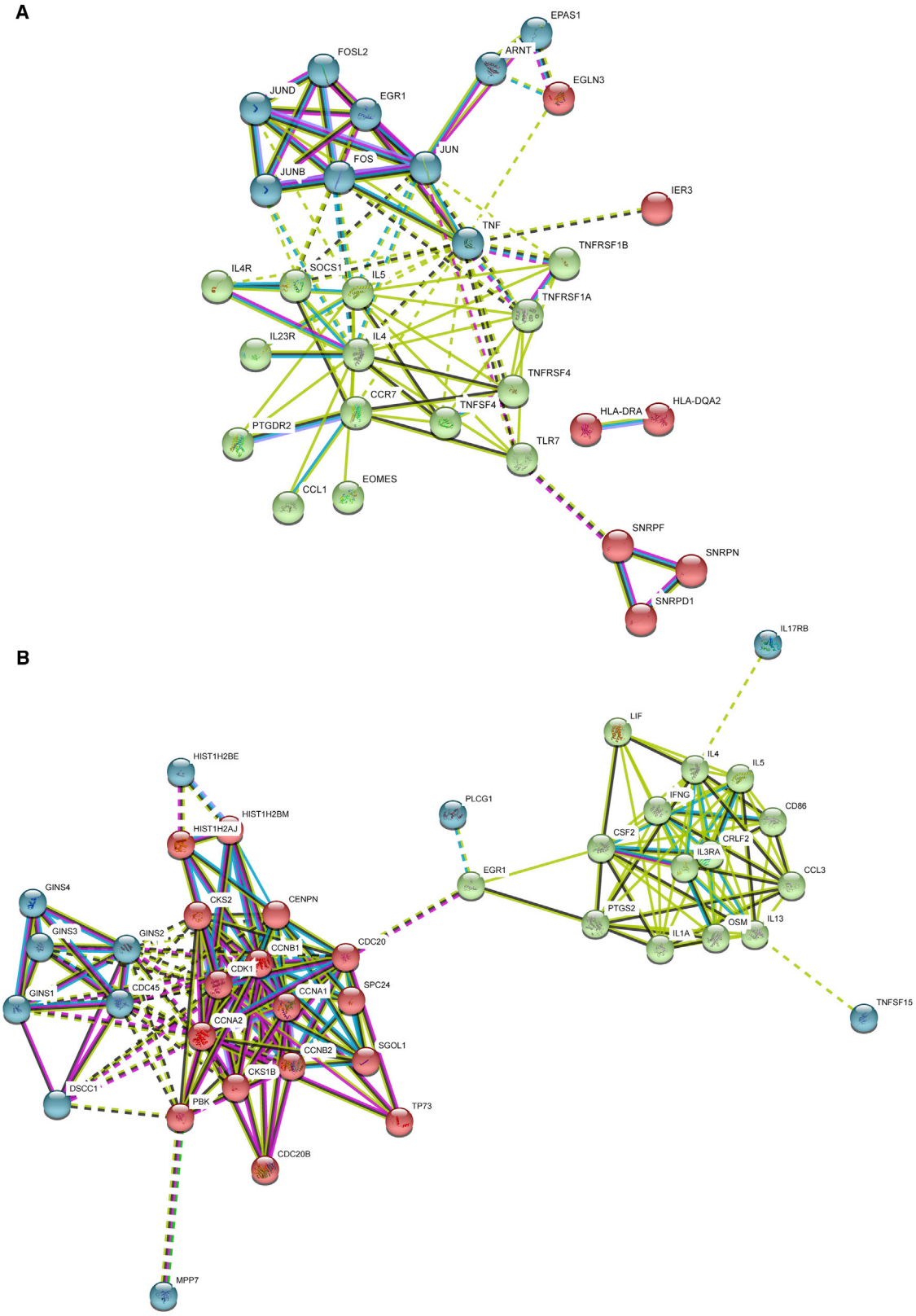

(legend on next page)

Table 1. Pathway Analysis Showing Over-representation of Gene Ontology Biological Process Terms Related to Inflammation and Cell Cycle in dnTGF-βRII-T2A-Pbbz PSMA CAR T Cells at Days 14 and 21 of Culture

Pathway ID	Pathway Description	Observed Gene Count	False Discovery Rate
Day 14			
GO.0034097	response to cytokine	14	8.87E−08
GO.0051707	response to other organism	14	8.87E−08
GO.1903708	positive regulation of hemopoiesis	9	9.32E−08
GO.1902107	positive regulation of leukocyte differentiation	8	4.32E−07
GO.0033993	response to lipid	13	3.61E−06
GO.0032496	response to lipopolysaccharide	9	5.37E−06
GO.0002639	positive regulation of immunoglobulin production	5	5.66E−06
GO.0006954	inflammatory response	10	1.01E−05
GO.0031347	regulation of defense response	12	1.19E−05
GO.0009617	response to bacterium	10	1.44E−05
Day 21			
GO.0000278	mitotic cell cycle	67	2.00E−34
GO.1903047	mitotic cell cycle process	57	1.46E−27
GO.0007049	cell cycle	72	7.91E−27
GO.0022402	cell cycle process	62	1.12E−24
GO.0007067	mitotic nuclear division	39	6.56E−24
GO.0051301	cell division	42	8.18E−22
GO.0000280	nuclear division	40	1.50E−21
GO.0048285	organelle fission	41	1.50E−21
GO.0007059	chromosome segregation	27	1.62E−18
GO.0051726	regulation of cell cycle	45	2.17E−13

The top 10 processes are listed; the complete list is shown in Table S3.

related to cytokine release. It is also possible that the weight loss was related to overexpression of LIF in the dnTGF-βRII-T2A-Pbbz CAR T cells,[28] a gene with >4-fold higher expression than in Pbbz CAR T cells with intact TGF signaling (Table S1). As in the first experiment, there were elevated levels of human CAR T cells found in the blood at days 33 and 64 in the high-dose dnTGF-βRII-T2A-Pbbz CAR T cell group, with associated signs of xGVHD at day 64 (Figure 5E).

To further determine mechanisms leading to enhanced proliferation and antitumor efficacy of CAR T cells that are expressing the dnTGF-βRII, we performed an additional *in vivo* experiment to investigate the effects of the dnTGF-βRII on T cell differentiation. Mice were randomized to T cell treatment groups within the same cage of mice to control for unforeseen variables affecting T cell engraftment and proliferation, weight loss, and GVHD. Using a protocol like that shown in Figure 4, mice were injected with 5×10^6 CAR T cells, and we included 10 mice per group in anticipation of needing to sacrifice animals to necropsy to investigate the GVHD (Figure 6A). Similar to the previous animal experiments, the dnTGF-βRII-T2A-Pbbz group had superior antitumor efficacy and controlled the tumors long-term, while the Pbbz group exhibited progressive cancer (Figures 6B and 6D).

Similar to the previous animal experiments, the dnTGF-βRII-T2A-Pbbz group had progressive weight loss and developed signs of xGVHD around day 35, with all of the mice requiring euthanasia at approximately day 42 (Figure 6C). Confirming previous experiments, there was a striking enhancement of CAR T cells in the dnTGF-βRII-T2A-Pbbz group of mice, as the mouse blood at day 35 contained approximately 25×10^6 human CAR T cells per mL of mouse blood compared to less than 1e6 CAR T cells per mL in the Pbbz T cell group. The CAR T cell lymphocytosis comprised both CD4+ and CD8+ T cells, with approximately a 2:1 CD4:CD8 ratio on day 35. Importantly, we found that the dnTGF-βRII-T2A-Pbbz mice had significantly higher levels of central memory $CD8^+$ T cells (Figure 6E). We did not observe any difference in the numbers of $FoxP3^+$ T cells within the blood of these mice.

DISCUSSION

Our results indicate that PSMA-specific, TGF-β-insensitive (dnTGF-βRII-T2A-Pbbz) CAR T cells can specifically eliminate advanced tumors that express PSMA. In addition, the PSMA-specific, TGF-β-insensitive CAR T cells have a striking proliferative advantage over wild-type PSMA CAR T cells that retain TGF-β signaling. These results have potential clinical utility, because all reported CAR T cell trials to date in patients with solid tumors have had disappointing CAR T cell expansion[7,8] that is several orders of magnitude that below CD19- and BCMA-specific CAR T cells employed for hematologic malignancies.[29,30]

From these long-term *in vitro* proliferation assays, we used multiple modalities to further characterize and interrogate the mechanisms for this enhanced proliferation upon TGF-β blockade. Most interestingly, we identified a distinct transcriptional program in the T cells expressing PSMA Pbbz CAR and the dnTGF-βRII-T2A-Pbbz CAR in the presence of TGF-β, as there were 329 genes or microRNAs (miRNAs) that were differentially expressed by >2-fold after 21 days of culture.

The dnTGF-βRII-T2A-Pbbz CAR T cells have enhanced cytokine signaling and secretion of a variety of cytokines that would be

Figure 3. Protein-Protein Interactions in PSMA dnTGF-βRII-T2A-Pbbz CAR T Cells

A protein-protein interaction network was constructed using STRING, version 10.5, based on differentially expressed genes on days 14 (A) and 21 (B) of culture. Network nodes represent proteins and the edges represent protein-protein interactions (physical or functional). In (A), the network has 43 nodes and 91 edges, with a p value of 1.3×10^{-14} compared to random interactions. In (B), the network has 69 nodes and 182 edges, with a p value of $<1.0 \times 10^{-16}$ compared to random interactions. The error bars represent ± SD.

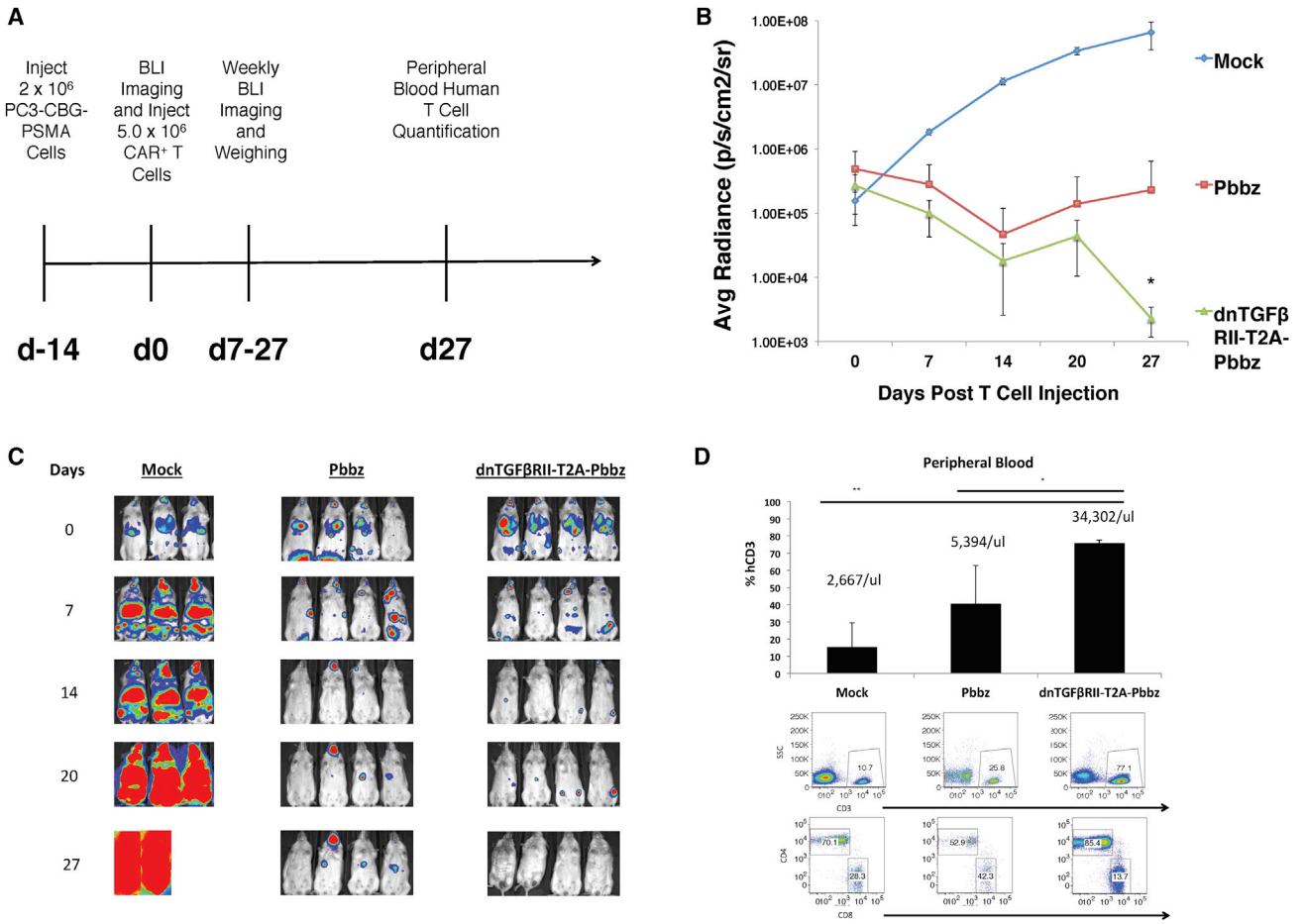

Figure 4. dnTGF-βRII-T2A-Pbbz CAR T Cells Have Augmented Proliferation and Eradicate Metastatic Prostate Cancer *In Vivo*

Systemic PC3-PSMA tumors were established by tail vein infusions of 2×10^6 tumor cells with the timeline described in (A) treated by infusing 5.0×10^6 CAR T cells or PBS (mock) per mouse 2 weeks later. Mice were assessed with bioluminescent imaging (BLI) weekly to assess tumor burden (B). Images of this BLI assessment are shown to demonstrate location and burden of tumors (C). Mice were bled at the end of the experiment at day 27 to assess the phenotype and the amounts of human CD3 T cells within the blood of these mice (D) (n = 4 mice/group). The error bars represent ± SD. *p < 0.05 and **p < 0.01, determined using a Student's two-tailed t test.

expected to enhance innate and acquired immunity. The cytokine profile demonstrates a balanced T_H2 phenotype with IL-4, IL-5, and IL-13 expression, as well as T_H1 phenotype with IL-2; IFN-γ; and chemokines MIP1-α, MIP1-β, and RANTES. In previous studies, CD4+ T cells and tumor cells engineered to secrete IL-4 have been shown to have potent antitumor effects.[31,32]

In addition to enhanced cytokine secretion, we identified the expression of a major network of genes associated with cell cycle progression and cell division, as well as increased expression of transcription factors associated with robust T cell effector functions. The pronounced differential expression of cell cycle genes was late to emerge after 21 days of culture. It is possible that this simply reflects continued proliferation of the dnTGF-βRII-T2A-Pbbz CAR T cells, while the PSMA Pbbz CAR T cells become progressively exhausted with decreased proliferation. Previous studies have reported that chronic stimulation of CAR T cells can lead to exhaustion, terminal differentiation, and apoptosis.[33,34] It is noteworthy that enhanced proliferation of the dnTGF-βRII-T2A-Pbbz CAR T cells was observed consistently *in vitro* and in all 3 *in vivo* experiments.

A third mechanism identified that may contribute to enhanced antitumor efficacy was a reduction of $CD4^+FoxP3^+$ cells that was observed after 21 days of co-culture with PC3-PSMA tumor cells. Along with an increase of $CD4^+$ central memory and $CD127^+$ T cells, these effects would be expected to contribute to enhanced CAR T cell proliferation.[35]

From the three animal experiments, it is evident that the dnTGF-βRII allows for enhanced antitumor responses when using the Pbbz CAR, allowing for tumor eradication and sustained long-term proliferation and persistence of the T cells. We found that the dnTGF-βRII gave much higher numbers of human T cells within the blood of these mice, correlating with substantial weight loss and GVHD. Most of

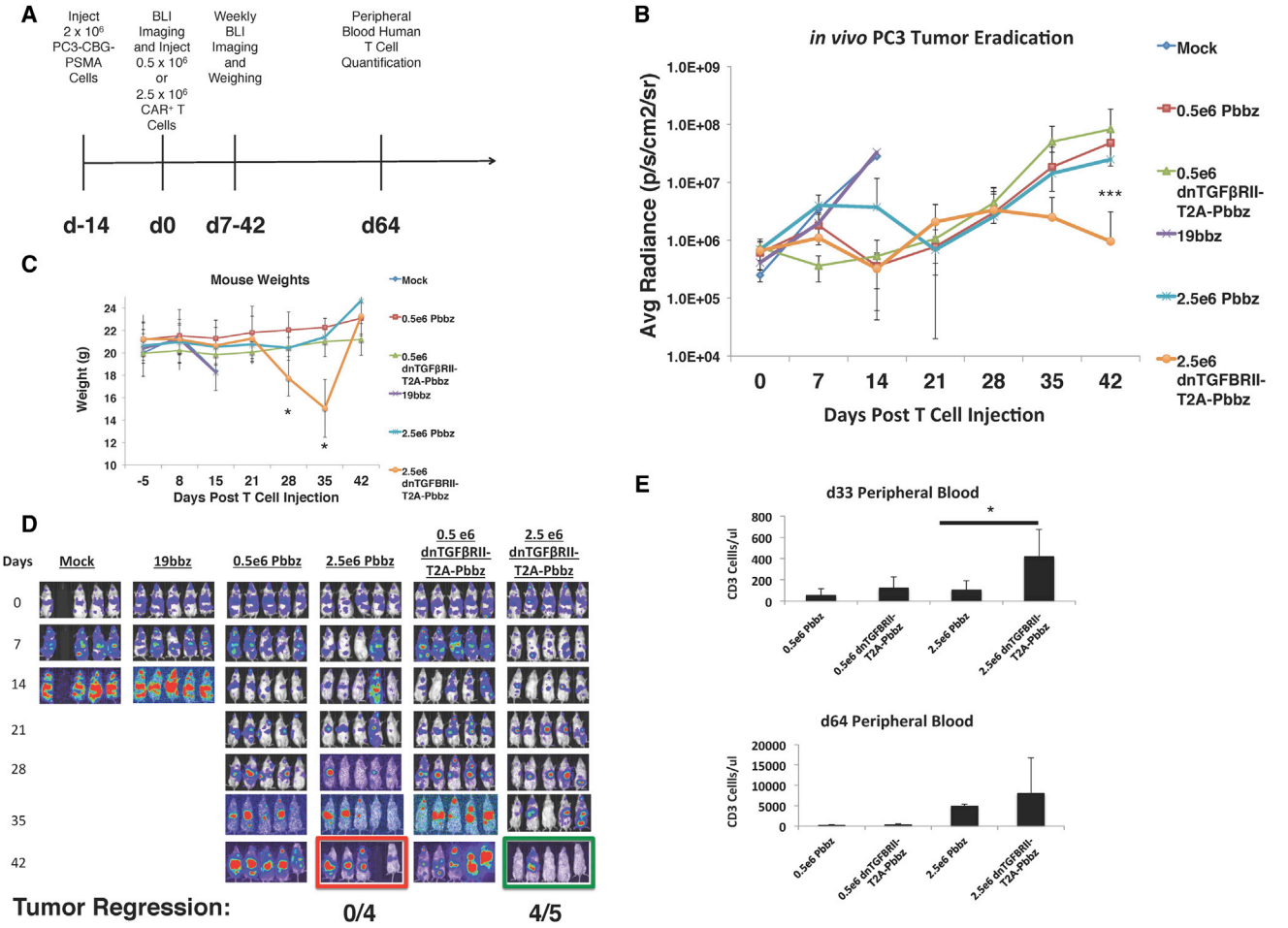

Figure 5. Dose-Dependent Augmentation of CAR T Cell Proliferation and Antitumor Efficacy of dnTGF-βRII CAR T Cells Compared to PSMA CAR T Cells *In Vivo*

Systemic PC3-PSMA tumors were established from intravenous (i.v.) infusions with the timeline described in (A), with varied doses of 0.5×10^6 and 2.5×10^6 CAR T cells per mouse infused 2 weeks later. Mice were assessed with BLI weekly to assess tumor burden (B). Body weight of the groups of mice is shown in (C). Images of this BLI assessment are shown to demonstrate location and burden of tumors (D). Mice were bled at days 33 and 64 to assess the amounts of human CD3 T cells within the blood of these mice (E) (n = 5 mice/group). The error bars represent ± SD. *$p < 0.05$ and ***$p < 0.001$.

the T cells were skewed to $CD4^+$ *in vivo*. Significantly higher amounts of $CD8^+$ central memory cells were observed with the dnTGF-βRII-T2A-Pbbz group. These toxic effects of the dnTGF-βRII-T2A-Pbbz CAR T cells are most likely due to enhanced xenogeneic effector functions of the CAR T cells.

A limitation of our approach is that the enhanced proliferation of the dnTGF-βRII-T2A-Pbbz CAR T cells could lead to a lymphoproliferative syndrome, as has been reported in mice.[20] To date, we have not observed antigen or growth factor-independent proliferation of dnTGF-βRII-T2A-Pbbz CAR T cells. A recent study has shown that mouse T cells can transform if haploinsufficient for PD-1.[36] It is possible that TGF-β has a similar cell-intrinsic tumor suppressor function in T cells. The immunodeficient mouse models that we and others in the field use have not generally predicted toxicities of CAR T cells, such as cytokine release syndrome or neurologic toxicity.[37–39]

Based on these encouraging preclinical results, we have initiated a clinical trial to infuse dnTGF-βRII-T2A-PBBZ CAR T cells in a first-in-human study in patients with refractory castration-resistant metastatic prostate cancer (ClinicalTrials.gov: NCT03089203). Through these investigations, we hope to learn better methods to sustain and augment CAR T cell proliferation and effector function in patients with advanced solid tumors.

MATERIALS AND METHODS

Vector Design

mRNA was isolated using the RNEasy Plus Mini Kit (QIAGEN) from human peripheral blood mononuclear cells (PBMCs) to produce

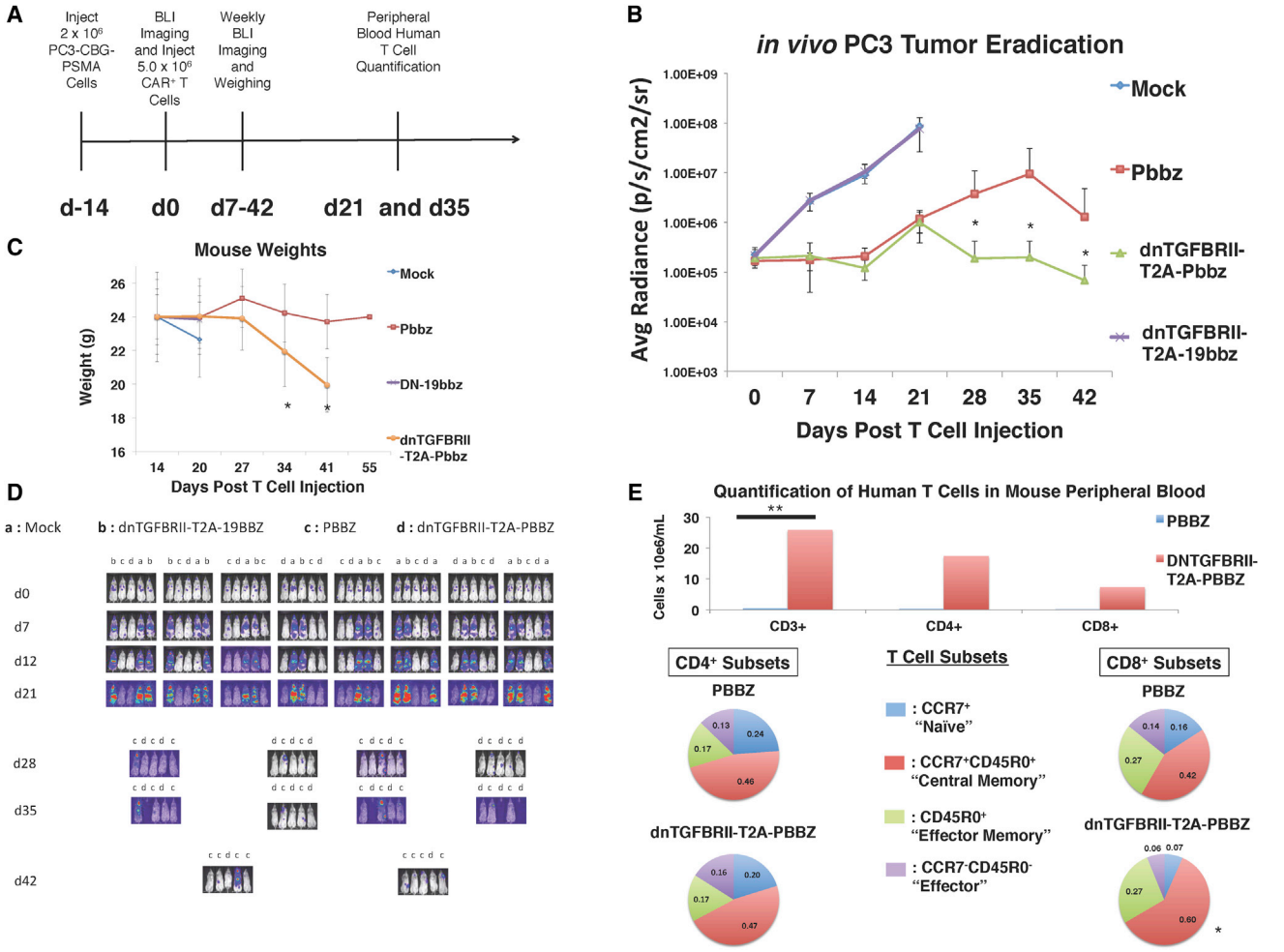

Figure 6. Enhanced Survival and Central Memory PSMA dnTGF-βRII-T2A-Pbbz CAR T Cells *In Vivo* in Mice with Metastatic Prostate Cancer

Systemic PC3-PSMA tumors were established by tail vein infusion with the timeline described in (A) with a dose of 5.0 × 10^6 CAR T cells per mouse infused 2 weeks later. Mice were assessed with BLI weekly to assess tumor burden (B). Body weight is shown in (C) and images of this BLI assessment are shown to demonstrate location and burden of tumors (D). (E) Mice were bled at the end of the experiment at day 35 to assess the amounts of human $CD3^+$ T cells within the blood of these mice. In depth analysis to assess T cell subsets was performed based on memory markers (CCR7, CD45R0, and CD127) (n = 10 mice/group). The error bars represent ± SD. *$p < 0.05$ and **$p < 0.01$.

cDNA using RETROscript cDNA kit (Ambion). Primers were designed to amplify the TGF-βRII transcript variant 2 (NM_003242), including a 5′ BspEI site and a 3′ NheI site. This was cloned into pELNS-tetR-T2A-Zeocin to replace the tetR cistron to form pELNS-TGF-βRII-T2A-Zeocin. Next, the TGF-βRII-T2A-Zeocin cassette was moved into the lentiviral expression plasmid from the Translational Research Program (pTRPE) lentiviral vector under the EF1alpha promoter utilizing the XbaI and SalI sites. A CAR was designed and synthesized by Geneart (Thermo Fisher Scientific) utilizing the variable light and heavy chains of the J591 antibody sequence from Dr. Neil Bander's (Weill Cornell Medical College) patent application (WO2002098897A2), fused to the 4-1BB intracellular domain sequence and CD3ζ intracellular domain sequences.[40] The dominant-negative TGF-βRII was constructed by truncating the human TGFBRII to remove the intracellular kinase domain at residue 199 as originally reported.[17] Synthesized CAR DNA was digested with XbaI and SalI and inserted into pTRPE-TGF-βRII-T2A-Zeocin utilizing the Avr2 and SalI sites.

Lentiviral Vector Production and CAR T Cell Production

Lentiviral supernatants were collected from tripartite-transfected HEK293T cells and concentrated using ultracentrifugation, as described by Resier et al.[41] These lentiviral vectors were used to transduce normal donor human T cells isolated from PBMCs using anti-CD4 and anti-CD8 microbeads (Miltenyi Biotec) and activated for 24 hr with anti-CD3/CD28 Dynabeads (Thermo Fisher Scientific). Transduced T cells were expanded for around 9 days in R10 media consisting of RPMI media (Gibco) with 10% fetal bovine serum

(FBS) (HyClone), 4-(2-hydroxyethyl)-1-piperazineethanesulfonic acid (HEPES), penicillin, and streptomycin with 30 U/mL IL-2. CAR T cells were then cryopreserved in 90% FBS and 10% DMSO for future use.

Cell Lines

The PC3 prostate cancer cell line, obtained from ATCC (CRL-1435), was isolated from a bone metastasis of a 62-year-old Caucasian with grade IV adenocarcinoma of the prostate. These cells grow to confluency *in vitro* within 3–4 days of being seeded at 1×10^4 cells/cm^2 and cultured in D10 media consisting of DMEM with 10% FBS (HyClone), HEPES, penicillin, and streptomycin. The tumor cell line was regularly validated to be Mycoplasma free, and it was authenticated in 2016 by the University of Arizona Genetics Core (Tucson, AZ). Using pTRPE vectors, we transduced these PC3 cells with lentiviral vectors to express click beetle green luciferase with GFP for easy quantification of lysis and *in vivo* tumor burden. We then used another pTRPE lentiviral vector to introduce the PSMA protein into these cells. These PC3 cells were sorted to 99% purity for the desired vectors using a BD FACS Aria II.

Flow Cytometry

A 4-laser LSRFortessa and a LSRII (Becton Dickinson) flow cytometer were used for analysis. Cells were stained in fluorescence-activated cell sorting (FACS) buffer (0.5% BSA Fraction V [Sigma], 2 mM EDTA [Life Technologies], in PBS [Life Technologies]) at 4°C for 30 min with the appropriate antibodies. For surface detection of the CAR, we used Jackson Laboratories Goat-anti-mouse PE-conjugated F(ab')2 (115-116-072) antibody. The R&D Systems TGF-βRII antibody antigen-presenting cell (APC) conjugate (FAB2411A) was used to detect the dnTGF-βRII. To detect phosphor-SMAD2/3, we used BD Phosflow antibodies (562586) with the recommended intracellular staining products and protocols (BD Biosciences). The following antibodies were used for T cell phenotyping: CD3-BV605, CD4-BV510, CD127-BV711 (BioLegend), CCR7-FITC, CD8-APCH7, CD45RO-PE (Becton Dickinson), FoxP3-PE, and Helios-PerCP-Cy5.5 (eBiosciences). For FoxP3 and Helios staining, the recommended intranuclear staining products and protocols were used (eBiosciences). To process mouse blood for flow cytometry, 50 of 65 μL blood retroorbitally drawn was lysed on ice for 5 min with 2 mL 1× RBC Lysis Buffer (BioLegend), centrifuged at 4°C for 5 min at 500 × *g*, washed twice with FACS buffer, and used for antibody staining. Countbright beads (Thermo Fisher Scientific) were used to determine the absolute number of cells per milliliter of blood.

TGF-β ELISA

To reduce the amount of background TGF-β present in FBS, we serum starved these cells at 0.5% FBS in order to determine the amount of TGF-β truly secreted by the tumor cell lines. Cells were cultured at 1e6 cells/well in 6-well plates for 24 hr and supernatants were harvested. To determine the amount of latent TGF-β secreted by tumor cell lines, the TGF-β ELISA kit (R&D Systems, DY240-05) was used to quantify the amount of TGF-β present in the supernatant. Undetectable amounts of mature TGF-β were observed, so supernatant samples were treated for 10 min at room temperature (RT) with 1N HCL and neutralized with 1N NaOH with 0.5 M HEPES to cleave latent TGF-β into mature TGF-β.

Tumor Lysis Assays

Since our PC3 cells were designed to express luciferase, the Promega Luciferase Reporter Assay System (E1910) was used to correlate luminescence to percentage cell lysis. By including tumor cells alone as 0% lysis and by completely lysing them in 0.01% Triton X-100 as 100% lysis, we established a sensitive method to detect percentage lysis of tumor cells by CAR T cells. After 16 hr of co-culture of PC3 cells with T cells at effector:target ratios from 0 to 25:1, cells were harvested, lysed, and luminescence was determined using the Promega system.

T Cell *In Vitro* Proliferation Assay

PC3 cells were irradiated with 15 Gy irradiation and plated at 0.2e6 cells per well of 12-well plates. 24 hr later, 1e6 T cells total were plated with the irradiated PC3 cells in R10 media without any IL-2 added in 2 mL media. Media were added as necessary, usually 4 days after plating if cell densities were over 1e6/mL and media were yellowing for 4 mL media/well total. 1e6 T cells from these cultures were taken and replated on freshly irradiated 0.2e6 PC3 cells, and this assay was continued with replating T cells on irradiated tumor cells every week. Cell numbers and size were evaluated using a Beckman Coulter Multisizer 3 Cell Counter.

Cytokine Analysis

Using the harvested supernatants 24 hr after plating co-cultures from these long-term proliferation assays, the human cytokine magnetic 30-Plex panel (Life Technologies LHC6003M) was used to quantify the following cytokines: IL-1RA, fibroblast growth factor (FGF)-basic, MCP-1, granulocyte colony-stimulating factor [G-CSF], IFN-γ, IL-12, IL-13, IL-7, granulocyte-macrophage colony-stimulating factor [GM-CSF], TNF-α, IL-1β, IL-2, IL-4, IL-5, IL-6, IFN-α, IL-15, IL-10, macrophage inflammatory protein [MIP]-1α, IL-17, IL-8, epidermal growth factor (EGF), human growth factor [HGF], vascular endothelial growth factor [VEGF], monokine induced by gamma IFN [MIG], RANTES, Eotaxin, MIP-1β, IFN-γ-induced protein 10 [IP-10], and IL-2R. Samples were measured on a FlexMAP 3D instrument (Luminex, Austin, TX) and evaluated with xPONENT software (Luminex).

Global Gene Expression Profiling

Live cells were isolated from the long-term proliferation cultures using a dead cell removal kit (Miltenyi 130-090-101), and whole RNA was isolated using RNeasy Mini Isolation Kit (QIAGEN 74104). These samples were isolated in triplicate at multiple time points and were submitted to the Molecular Profiling Core Facility at the University of Pennsylvania. These samples were run on Human GeneChip Microarray 2.0 ST microarrays (Thermo Fisher Scientific), and analysis was performed using Transcriptome and Expression Analysis Console (Thermo Fisher Scientific). DEGs that were significant ($p < 0.05$) were uploaded into STRING version (v.)10.5 *Homo*

sapiens,[27] which clusters genes into networks based on scored interactions, associations, and pathway knowledge drawn from databases such as KEGG and Gene Ontology and text mined from PubMed literature. Networks were constructed where the network edges were based on a minimum interaction confidence of 0.4, a maximum of 10 interactors, and the interaction sources were as follows: text-mining, experiments, databases, co-expression, neighborhood, gene fusion, and co-occurrence.

Animal Experiments

The University of Pennsylvania Institutional Animal Care and Use Committee approved all animal experiments. Female NSG knockout (KO) mice were provided and housed by the University of Pennsylvania Stem Cell and Xenograft core. Using 200 μL 1× PBS, 2e6 PC3-PSMA cells were injected intravenously via the tail vein. Tumors were established systemically for 2 weeks, upon which CAR T cells were then injected at various doses in the same manner. Bioluminescence imaging was performed by injecting mice weekly intraperitoneally with luciferin and quantifying luminescence using a Xenogen IVIS-200 Spectrum imaging system. Blood was drawn using glass capillary tubes from the retroorbital sinus. All experiments were performed via protocols approved by the Institutional Animal Care and Use Committee of the University of Pennsylvania.

Statistics

All statistical analysis was performed using GraphPad Prism v.6 (GraphPad Software Inc.). For comparisons of 2 groups, 2-tailed unpaired t tests were used. Correlation was estimated by calculation of 2-tailed Pearson coefficients and significance. Data were transformed when needed to normalize variance. Power analysis was conducted using software as reported.[42] Symbols indicate statistical significance as follows: *$p < 0.05$, **$p < 0.01$, and ***$p < 0.005$.

SUPPLEMENTAL INFORMATION

Supplemental Information includes one figure and three tables and can be found with this article online at https://doi.org/10.1016/j.ymthe.2018.05.003.

AUTHOR CONTRIBUTIONS

C.C.K. designed and performed experiments, analyzed data, interpreted results, and wrote the manuscript. J.L. contributed reagents, designed and performed experiments, and analyzed data. A.Z. and F.C. performed experiments. J.J.M. and S.F.L. designed experiments, interpreted results, and edited the manuscript. M.V.M. and Y.Z. designed experiments and interpreted results. J.A.F. contributed reagents, designed and performed experiments, analyzed data, interpreted results, and edited the manuscript. C.H.J. designed experiments, analyzed data, interpreted results, and wrote the manuscript.

CONFLICTS OF INTEREST

Y.Z. submitted a patent application related to this work. The authors have sponsored research support from Tmunity.

ACKNOWLEDGMENTS

This work was supported by grants from the Prostate Cancer Foundation to M.V.M., Y.Z., and C.H.J. and Young Investigator Awards to C.C.K. and J.L.

REFERENCES

1. Litwin, M.S., and Tan, H.J. (2017). The Diagnosis and Treatment of Prostate Cancer: A Review. JAMA *317*, 2532–2542.
2. Kwon, E.D., Drake, C.G., Scher, H.I., Fizazi, K., Bossi, A., van den Eertwegh, A.J., Krainer, M., Houede, N., Santos, R., Mahammedi, H., et al.; CA184-043 Investigators (2014). Ipilimumab versus placebo after radiotherapy in patients with metastatic castration-resistant prostate cancer that had progressed after docetaxel chemotherapy (CA184-043): a multicentre, randomised, double-blind, phase 3 trial. Lancet Oncol. *15*, 700–712.
3. Chen, D.S., and Mellman, I. (2017). Elements of cancer immunity and the cancer-immune set point. Nature *541*, 321–330.
4. Huang, A.C., Postow, M.A., Orlowski, R.J., Mick, R., Bengsch, B., Manne, S., Xu, W., Harmon, S., Giles, J.R., Wenz, B., et al. (2017). T-cell invigoration to tumour burden ratio associated with anti-PD-1 response. Nature *545*, 60–65.
5. Verdegaal, E.M., de Miranda, N.F., Visser, M., Harryvan, T., van Buuren, M.M., Andersen, R.S., Hadrup, S.R., van der Minne, C.E., Schotte, R., Spits, H., et al. (2016). Neoantigen landscape dynamics during human melanoma-T cell interactions. Nature *536*, 91–95.
6. June, C.H., Warshauer, J.T., and Bluestone, J.A. (2017). Is autoimmunity the Achilles' heel of cancer immunotherapy? Nat. Med. *23*, 540–547.
7. Sadelain, M., Rivière, I., and Riddell, S. (2017). Therapeutic T cell engineering. Nature *545*, 423–431.
8. Lim, W.A., and June, C.H. (2017). The Principles of Engineering Immune Cells to Treat Cancer. Cell *168*, 724–740.
9. Rabinovich, G.A., Gabrilovich, D., and Sotomayor, E.M. (2007). Immunosuppressive strategies that are mediated by tumor cells. Annu. Rev. Immunol. *25*, 267–296.
10. Joyce, J.A., and Fearon, D.T. (2015). T cell exclusion, immune privilege, and the tumor microenvironment. Science *348*, 74–80.
11. Chong, E.A., Melenhorst, J.J., Lacey, S.F., Ambrose, D.E., Gonzalez, V., Levine, B.L., June, C.H., and Schuster, S.J. (2017). PD-1 blockade modulates chimeric antigen receptor (CAR)-modified T cells: refueling the CAR. Blood *129*, 1039–1041.
12. Condomines, M., Arnason, J., Benjamin, R., Gunset, G., Plotkin, J., and Sadelain, M. (2015). Tumor-Targeted Human T Cells Expressing CD28-Based Chimeric Antigen Receptors Circumvent CTLA-4 Inhibition. PLoS ONE *10*, e0130518.
13. Siegel, P.M., and Massagué, J. (2003). Cytostatic and apoptotic actions of TGF-β in homeostasis and cancer. Nat. Rev. Cancer *3*, 807–821.
14. Hanahan, D., and Weinberg, R.A. (2011). Hallmarks of cancer: the next generation. Cell *144*, 646–674.
15. Travis, M.A., and Sheppard, D. (2014). TGF-β activation and function in immunity. Annu. Rev. Immunol. *32*, 51–82.
16. Ebner, R., Chen, R.H., Shum, L., Lawler, S., Zioncheck, T.F., Lee, A., Lopez, A.R., and Derynck, R. (1993). Cloning of a type I TGF-beta receptor and its effect on TGF-beta binding to the type II receptor. Science *260*, 1344–1348.
17. Wieser, R., Attisano, L., Wrana, J.L., and Massagué, J. (1993). Signaling activity of transforming growth factor beta type II receptors lacking specific domains in the cytoplasmic region. Mol. Cell. Biol. *13*, 7239–7247.
18. Gorelik, L., and Flavell, R.A. (2001). Immune-mediated eradication of tumors through the blockade of transforming growth factor-beta signaling in T cells. Nat. Med. *7*, 1118–1122.
19. Gorelik, L., and Flavell, R.A. (2000). Abrogation of TGFbeta signaling in T cells leads to spontaneous T cell differentiation and autoimmune disease. Immunity *12*, 171–181.
20. Lucas, P.J., Kim, S.J., Melby, S.J., and Gress, R.E. (2000). Disruption of T cell homeostasis in mice expressing a T cell-specific dominant negative transforming growth factor beta II receptor. J. Exp. Med. *191*, 1187–1196.

21. Zhang, Q., Yang, X., Pins, M., Javonovic, B., Kuzel, T., Kim, S.J., Parijs, L.V., Greenberg, N.M., Liu, V., Guo, Y., and Lee, C. (2005). Adoptive transfer of tumor-reactive transforming growth factor-beta-insensitive CD8+ T cells: eradication of autologous mouse prostate cancer. Cancer Res. *65*, 1761–1769.

22. Donkor, M.K., Sarkar, A., Savage, P.A., Franklin, R.A., Johnson, L.K., Jungbluth, A.A., Allison, J.P., and Li, M.O. (2011). T cell surveillance of oncogene-induced prostate cancer is impeded by T cell-derived TGF-β1 cytokine. Immunity *35*, 123–134.

23. Foster, A.E., Dotti, G., Lu, A., Khalil, M., Brenner, M.K., Heslop, H.E., Rooney, C.M., and Bollard, C.M. (2008). Antitumor activity of EBV-specific T lymphocytes transduced with a dominant negative TGF-beta receptor. J. Immunother. *31*, 500–505.

24. Bollard, C.M., Tripic, T., Cruz, C.R., Dotti, G., Gottschalk, S., Torrano, V., Dakhova, O., Carrum, G., Ramos, C.A., Liu, H., et al. (2018). Tumor-Specific T-Cells Engineered to Overcome Tumor Immune Evasion Induce Clinical Responses in Patients With Relapsed Hodgkin Lymphoma. J. Clin. Oncol. *36*, 1128–1139.

25. Vallabhajosula, S., Nikolopoulou, A., Jhanwar, Y.S., Kaur, G., Tagawa, S.T., Nanus, D.M., Bander, N.H., and Goldsmith, S.J. (2016). Radioimmunotherapy of Metastatic Prostate Cancer with ^{177}Lu-DOTAhuJ591 Anti Prostate Specific Membrane Antigen Specific Monoclonal Antibody. Curr. Radiopharm. *9*, 44–53.

26. Bander, N.H., Trabulsi, E.J., Kostakoglu, L., Yao, D., Vallabhajosula, S., Smith-Jones, P., Joyce, M.A., Milowsky, M., Nanus, D.M., and Goldsmith, S.J. (2003). Targeting metastatic prostate cancer with radiolabeled monoclonal antibody J591 to the extracellular domain of prostate specific membrane antigen. J. Urol. *170*, 1717–1721.

27. Szklarczyk, D., Franceschini, A., Wyder, S., Forslund, K., Heller, D., Huerta-Cepas, J., Simonovic, M., Roth, A., Santos, A., Tsafou, K.P., et al. (2015). STRING v10: protein-protein interaction networks, integrated over the tree of life. Nucleic Acids Res. *43*, D447–D452.

28. Beretta, E., Dhillon, H., Kalra, P.S., and Kalra, S.P. (2002). Central LIF gene therapy suppresses food intake, body weight, serum leptin and insulin for extended periods. Peptides *23*, 975–984.

29. Kalos, M., Levine, B.L., Porter, D.L., Katz, S., Grupp, S.A., Bagg, A., and June, C.H. (2011). T cells with chimeric antigen receptors have potent antitumor effects and can establish memory in patients with advanced leukemia. Sci. Transl. Med. *3*, 95ra73.

30. Ali, S.A., Shi, V., Maric, I., Wang, M., Stroncek, D.F., Rose, J.J., Brudno, J.N., Stetler-Stevenson, M., Feldman, S.A., Hansen, B.G., et al. (2016). T cells expressing an anti-B-cell maturation antigen chimeric antigen receptor cause remissions of multiple myeloma. Blood *128*, 1688–1700.

31. Golumbek, P.T., Lazenby, A.J., Levitsky, H.I., Jaffee, L.M., Karasuyama, H., Baker, M., and Pardoll, D.M. (1991). Treatment of established renal cancer by tumor cells engineered to secrete interleukin-4. Science *254*, 713–716.

32. Hung, K., Hayashi, R., Lafond-Walker, A., Lowenstein, C., Pardoll, D., and Levitsky, H. (1998). The central role of CD4(+) T cells in the antitumor immune response. J. Exp. Med. *188*, 2357–2368.

33. Long, A.H., Haso, W.M., Shern, J.F., Wanhainen, K.M., Murgai, M., Ingaramo, M., Smith, J.P., Walker, A.J., Kohler, M.E., Venkateshwara, V.R., et al. (2015). 4-1BB costimulation ameliorates T cell exhaustion induced by tonic signaling of chimeric antigen receptors. Nat. Med. *21*, 581–590.

34. Frigault, M.J., Lee, J., Basil, M.C., Carpenito, C., Motohashi, S., Scholler, J., Kawalekar, O.U., Guedan, S., McGettigan, S.E., Posey, A.D., Jr., et al. (2015). Identification of chimeric antigen receptors that mediate constitutive or inducible proliferation of T cells. Cancer Immunol. Res. *3*, 356–367.

35. Lee, J.C., Hayman, E., Pegram, H.J., Santos, E., Heller, G., Sadelain, M., and Brentjens, R. (2011). In vivo inhibition of human CD19-targeted effector T cells by natural T regulatory cells in a xenotransplant murine model of B cell malignancy. Cancer Res. *71*, 2871–2881.

36. Wartewig, T., Kurgyis, Z., Keppler, S., Pechloff, K., Hameister, E., Öllinger, R., Maresch, R., Buch, T., Steiger, K., Winter, C., et al. (2017). PD-1 is a haploinsufficient suppressor of T cell lymphomagenesis. Nature *552*, 121–125.

37. Gust, J., Hay, K.A., Hanafi, L.A., Li, D., Myerson, D., Gonzalez-Cuyar, L.F., Yeung, C., Liles, W.C., Wurfel, M., Lopez, J.A., et al. (2017). Endothelial Activation and Blood-Brain Barrier Disruption in Neurotoxicity after Adoptive Immunotherapy with CD19 CAR-T Cells. Cancer Discov. *7*, 1404–1419.

38. Fitzgerald, J.C., Weiss, S.L., Maude, S.L., Barrett, D.M., Lacey, S.F., Melenhorst, J.J., Shaw, P., Berg, R.A., June, C.H., Porter, D.L., et al. (2017). Cytokine Release Syndrome After Chimeric Antigen Receptor T Cell Therapy for Acute Lymphoblastic Leukemia. Crit. Care Med. *45*, e124–e131.

39. Maude, S., and Barrett, D.M. (2016). Current status of chimeric antigen receptor therapy for haematological malignancies. Br. J. Haematol. *172*, 11–22.

40. Milone, M.C., Fish, J.D., Carpenito, C., Carroll, R.G., Binder, G.K., Teachey, D., Samanta, M., Lakhal, M., Gloss, B., Danet-Desnoyers, G., et al. (2009). Chimeric receptors containing CD137 signal transduction domains mediate enhanced survival of T cells and increased antileukemic efficacy in vivo. Mol. Ther. *17*, 1453–1464.

41. Kutner, R.H., Zhang, X.Y., and Reiser, J. (2009). Production, concentration and titration of pseudotyped HIV-1-based lentiviral vectors. Nat. Protoc. *4*, 495–505.

42. Dupont, W.D., and Plummer, W.D., Jr. (1998). Power and sample size calculations for studies involving linear regression. Control. Clin. Trials *19*, 589–601.

YMTHE, Volume *26*

Supplemental Information

Dominant-Negative TGF-β Receptor Enhances PSMA-Targeted Human CAR T Cell Proliferation And Augments Prostate Cancer Eradication

Christopher C. Kloss, Jihyun Lee, Aaron Zhang, Fang Chen, Jan Joseph Melenhorst, Simon F. Lacey, Marcela V. Maus, Joseph A. Fraietta, Yangbing Zhao, and Carl H. June

<u>Supplemental Figure 1.</u> Whole transcriptome microarray hierarchical clustergram analysis of dnTGFβRII expressing PSMA CAR T cells. Total live T cell mRNA was analyzed after 7 days (**A**), 14 days (**B**), and 21 days (**C**) of PC3-PSMA tumor cell coculture with T cells from 1) PBBZ group (Orange) or 2) PBBZ + dnTGFβRII (Green). Clustergram analysis clusters significantly differentially expressed genes into similar pathways. The scalebar indicates the level expression of individual genes.

A D7 Pbbz vs. dnTGFBRII-T2A-Pbbz

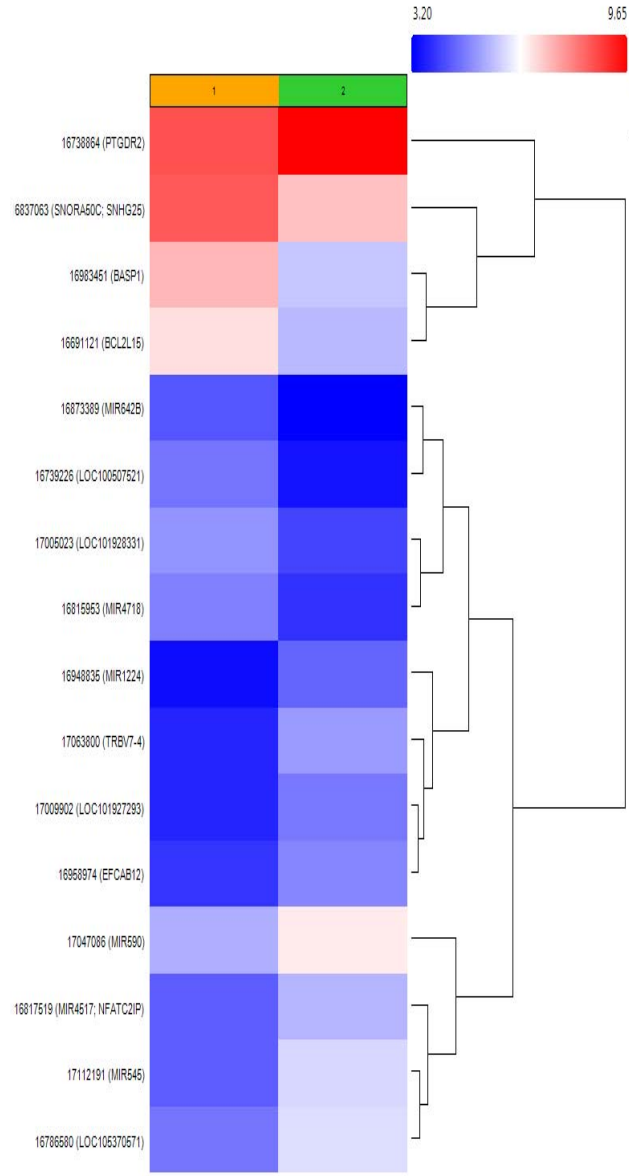

B D14 Pbbz vs. dnTGFBRII-T2A-Pbbz

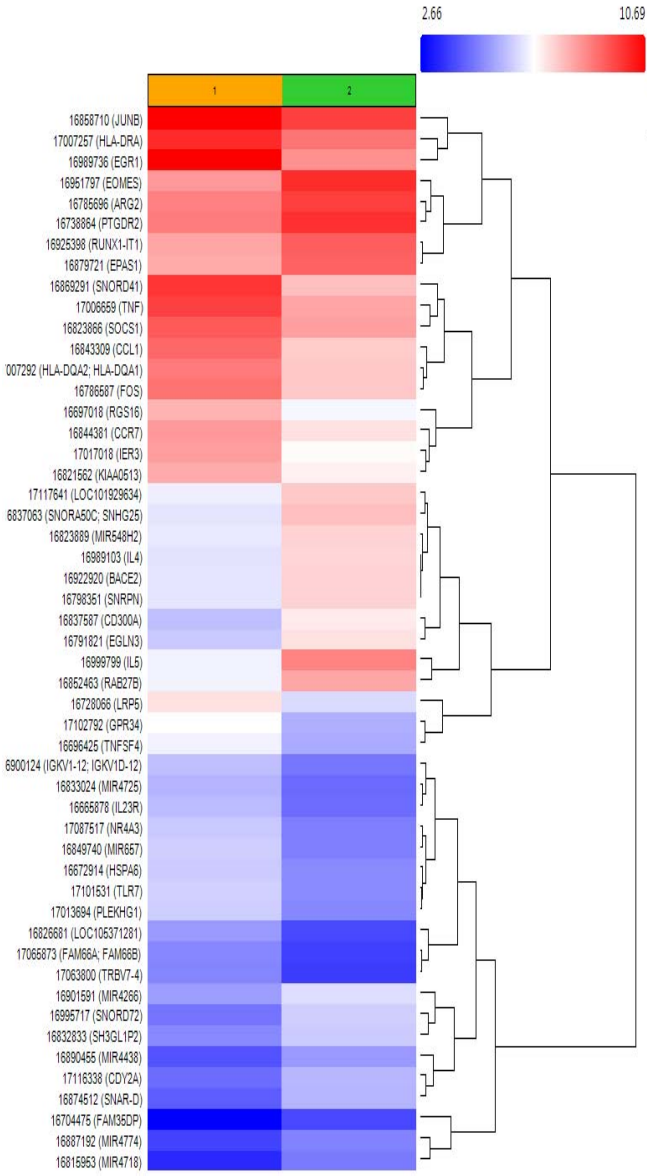

C D21 Pbbz vs. dnTGFBRII-T2A-Pbbz

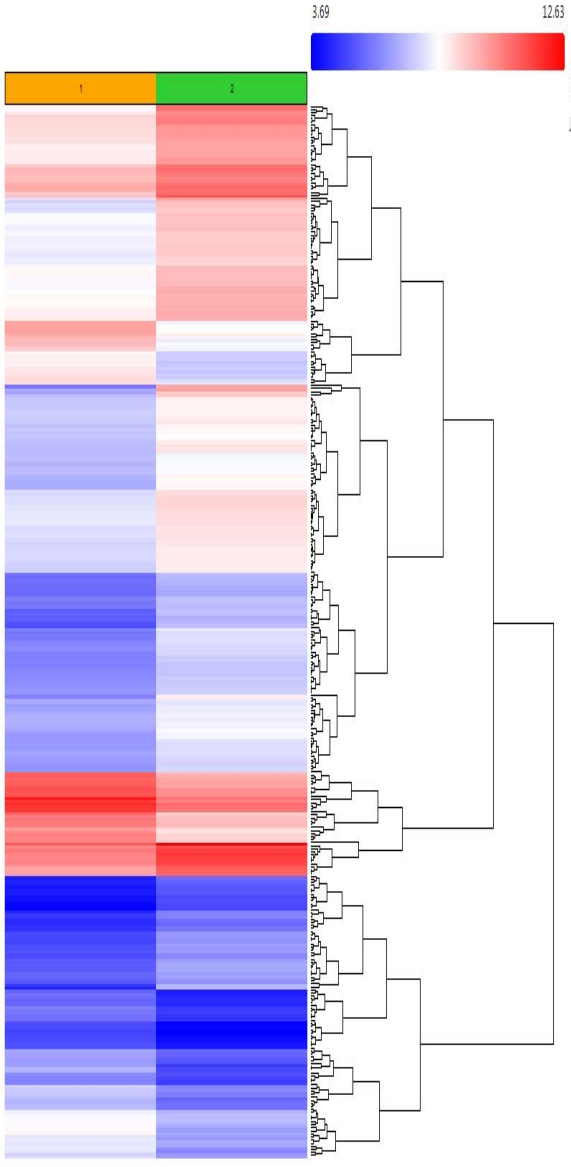

Supplemental Table 1.

Day 7			Day 14			Day 21		
Gene/MIR #	Fold Change	Gene Symbol	Gene/MIR #	Fold Change	Gene Symbol	Gene/MIR #	Fold Change	Gene Symbol
1	2.98	MIR545	1	4.46	IL5	1	15.05	IL5
2	2.87	TRBV7-4	2	3.24	EOMES	2	8.81	IL13
3	2.51	LOC105370571	3	2.98	RAB27B	3	6.29	APOD
4	2.39	MIR590	4	2.71	SNORD72	4	5.91	IL4
5	2.19	MIR4517; NFATC2IP	5	2.68	SNAR-D	5	5.39	EGR1
6	2.17	MIR1224	6	2.63	SNORA50C; SNHG25	6	5.07	EPAS1
7	2.08	LOC101927293	7	2.52	CD300A	7	4.63	SLCO4C1
8	2.04	PTGDR2	8	2.5	EGLN3	8	4.44	LIF
9	2.04	EFCAB12	9	2.45	MIR4718	9	4.35	RAB27B
10	-2.01	LOC101928331	10	2.28	PTGDR2	10	4.03	LOC101928173
11	-2.03	MIR4718	11	2.28	CDY2A	11	3.96	IFNG
12	-2.15	MIR642B	12	2.2	MIR4438	12	3.9	SLC7A8
13	-2.36	LOC100507521	13	2.2	FAM35DP	13	3.76	RNU5D-1
14	-2.43	BCL2L15	14	2.19	EPAS1	14	3.57	DUSP6
15	-2.51	SNORA50C; SNHG25	15	2.15	IL4	15	3.57	OSM
16	-3.09	BASP1	16	2.15	BACE2	16	3.49	TNFSF15
			17	2.15	SNRPN	17	3.48	CSF2
			18	2.12	RUNX1-IT1	18	3.33	LOC100505478
			19	2.12	LOC101929634	19	3.27	IL3RA
			20	2.07	MIR548H2	20	3.25	IL17RB
			21	2.05	MIR4774	21	3.21	GINS2
			22	2.04	SH3GL1P2	22	3.2	IL3RA
			23	2.03	ARG2	23	3.2	FAM72D; FAM72C
			24	2.02	MIR4266	24	3.2	PTGS2
			25	-2.01	HSPA6	25	3.17	TP73
			26	-2.04	JUNB	26	3.15	ARG2
			27	-2.04	LRP5	27	3.15	HIST1H2BE
			28	-2.07	SOCS1	28	3.07	CCNA1
			29	-2.14	TLR7	29	3.07	IL1A
			30	-2.16	TNFSF4 (AKA OX40	30	3.03	IFI30
			31	-2.16	KIAA0513	31	3.03	HIST1H2BM
			32	-2.18	CCR7	32	3.01	MCOLN3
			33	-2.18	FAM66A; FAM66B	33	2.99	HIST1H2AJ
			34	-2.19	PLEKHG1	34	2.98	CENPN
			35	-2.22	HLA-DRA	35	2.98	DSCC1
			36	-2.24	IGKV1-12; IGKV1D-12	36	2.97	CCL3
			37	-2.25	NR4A3	37	2.92	CRLF2
			38	-2.26	TRBV7-4	38	2.84	CPM
			39	-2.29	HLA-DQA2; HLA-DQA1	39	2.81	CDC20B
			40	-2.32	MIR4725	40	2.78	GPAT3
			41	-2.37	IL23R	41	2.78	CD86
			42	-2.38	MIR657	42	2.78	PBK
			43	-2.38	GPR34	43	2.77	FAM72A
			44	-2.44	LOC105371281	44	2.77	MT1G
			45	-2.5	RGS16	45	2.76	APOO
			46	-2.51	FOS	46	2.73	RNVU1-14
			47	-2.78	IER3	47	2.71	LOC100240735
			48	-2.87	CCL1	48	2.7	SPC24
			49	-2.95	TNF	49	2.7	SGOL1
			50	-4.48	SNORD41	50	2.68	CDK1
			51	-4.76	EGR1	51	2.68	MIR221
						52	2.67	CCL3L3; CCL3L1
						53	2.65	UBE2T
						54	2.64	SAMD5
						55	2.62	PTPN14
						56	2.61	CLECL1
						57	2.61	CDC20
						58	2.61	CDC6
						59	2.6	HPGDS
						60	2.6	CDKN3

61	2.6	TK1
62	2.6	OSBPL6
63	2.58	ITGA11
64	2.57	ASF1B
65	2.57	GUCY1B3
66	2.55	CCL1
67	2.55	CLSPN
68	2.55	HIST1H3H
69	2.55	HIST1H3G
70	2.54	SHCBP1
71	2.54	SPC25
72	2.54	LRRCC1
73	2.53	SPAG5
74	2.53	GINS4
75	2.5	TRAV9-1
76	2.5	C17orf58
77	2.5	DMC1
78	2.5	RPL39L
79	2.49	PLK1
80	2.48	PLPP1
81	2.48	CSAG3; CSAG2
82	2.48	CSAG3; CSAG2
83	2.48	SIGLEC17P
84	2.48	IFITM3
85	2.48	SKA1
86	2.48	HIST1H2AI
87	2.47	HBEGF
88	2.47	MTFR2
89	2.46	LOC105375905
90	2.46	HIST1H3J
91	2.44	CCNB1
92	2.43	DEPDC1
93	2.42	IL1RL1
94	2.42	GZMK
95	2.41	EXO1
96	2.41	CEP55
97	2.41	FOSL1
98	2.4	MYBL1
99	2.38	MYBL2
100	2.38	CCNE2
101	2.37	ESCO2
102	2.36	DTL
103	2.36	CENPW
104	2.35	KIF14
105	2.35	HIST1H4B
106	2.35	CDR1
107	2.33	LINC01123
108	2.33	MT2A
109	2.33	TNF
110	2.32	GAB2
111	2.32	RAD54L
112	2.32	SOCS1
113	2.32	CRNDE
114	2.32	NQO1
115	2.31	STX3; OR10Y1P
116	2.31	XRCC2
117	2.3	PMCH
118	2.3	CCL4L2; CCL4L1
119	2.29	MYO1B
120	2.28	BACE2
121	2.28	SMAGP
122	2.28	CCNB2
123	2.27	LOC101928865
124	2.27	GZMB

125	2.27	KIAA0101
126	2.27	SIGLEC6
127	2.27	CENPU
128	2.27	CENPH
129	2.27	HIST1H2BF
130	2.26	FAM111B
131	2.25	SPP1
132	2.25	LOC105370594
133	2.24	FOXM1
134	2.24	TUBA1B; TUBA1A
135	2.24	CCL4
136	2.24	KIR3DL2; KIR3DL1
137	2.23	ZWINT
138	2.23	SKA3
139	2.23	LINC01106
140	2.23	CDC45
141	2.23	DTHD1
142	2.23	HMGN5
143	2.22	TYMS
144	2.22	MAD2L1
145	2.22	HIST1H2BL
146	2.21	TOM1L1
147	2.21	CREG1
148	2.21	KLF5
149	2.21	HIST1H1B
150	2.21	ANLN
151	2.21	CLU; MIR6843
152	2.2	KLHL11
153	2.2	FCER1G
154	2.2	ORC1
155	2.2	MIR3665
156	2.19	TRBV7-4
157	2.19	SPOCK1
158	2.19	PRR11
159	2.19	RRM2
160	2.19	UBE2C
161	2.18	ORC6
162	2.17	ICAM1
163	2.17	STX11
164	2.17	CD9
165	2.17	MCM10
166	2.17	HIST1H3F
167	2.17	MELK
168	2.16	GAS2L3
169	2.16	NPC2; MIR4709
170	2.16	LOC105371152
171	2.16	DONSON
172	2.15	PDLIM5
173	2.15	RAB23
174	2.14	KCCAT198
175	2.14	CCNE1
176	2.14	KIF20A
177	2.14	DEPDC1B
178	2.13	NDC80
179	2.12	TMPO-AS1
180	2.12	KIF23
181	2.12	TPMT
182	2.11	DCLRE1B
183	2.11	PLA2G4A
184	2.11	DLGAP5
185	2.1	CDCA8
186	2.1	NUF2
187	2.1	ESPL1
188	2.1	TICRR

189	2.1	HMMR
190	2.1	CENPQ
191	2.09	NEK2
192	2.09	DIAPH3
193	2.09	RAD51
194	2.09	BIRC5
195	2.09	RNF130
196	2.09	SPAG1
197	2.08	FEN1; FADS2
198	2.07	BRCA2
199	2.07	GINS1
200	2.06	TLCD2
201	2.06	BCRP3
202	2.06	NCAPH
203	2.05	CDC7
204	2.05	GATA3-AS1
205	2.05	EME1
206	2.05	PSMC3IP
207	2.05	TMEM237
208	2.05	ECT2
209	2.05	TTK
210	2.04	YES1
211	2.04	ANPEP
212	2.04	RFC5
213	2.04	CLN6
214	2.04	CDT1
215	2.04	PMAIP1
216	2.04	BHLHE40-AS1
217	2.04	NCAPG
218	2.04	MND1
219	2.04	CCNA2
220	2.04	TRGV3; TRGC2
221	2.03	ETV7
222	2.03	AURKB
223	2.03	TLR3
224	2.02	CLEC7A
225	2.02	IRX3
226	2.02	RNVU1-3
227	2.02	RNVU1-3
228	2.02	TMTC1
229	2.02	CD200
230	2.02	PEX5L
231	2.02	SLC7A11
232	2.02	CENPP
233	2.01	CDCA5
234	2.01	E2F7
235	2.01	GOLGA8J
236	2.01	CDCA2
237	-2.01	SNORD61; RBMX
238	-2.01	KLRC2; KLRC3
239	-2.02	GUSBP3
240	-2.03	PLCG1; RPL23AP81
241	-2.03	TAS2R31
242	-2.03	SNORD116-6
243	-2.04	RNU6-82P
244	-2.04	SNORD116-19; SNORD116-17 SNORD116-19; SNORD116-17;
245	-2.04	SNRPN; IPW
246	-2.04	USP6
247	-2.06	PWAR5; SNORD108
248	-2.06	ERMN
249	-2.06	MIR1234; CPSF1
250	-2.07	PPIAL4E; PPIAL4D; PPIAL4F

251	-2.07	SNORD116-2
252	-2.08	POM121L8P
253	-2.09	ABLIM1
254	-2.1	SNORA12
255	-2.1	SORL1
256	-2.1	SCARNA11
257	-2.1	CCDC141
258	-2.11	LOC105371220
259	-2.11	PLXNA4
260	-2.12	IGKV1-12; IGKV1D-12
261	-2.12	CD44
262	-2.12	RNU4ATAC
263	-2.12	SNORA9; SNHG15
264	-2.13	SNORA50A
265	-2.13	MIR766
266	-2.15	B3GALT2
267	-2.15	DPRXP4
268	-2.17	SPNS3
269	-2.17	GPR155
270	-2.17	MIR4253
271	-2.17	KRT16P3
272	-2.17	LOC100128751
273	-2.18	ANKRD44-IT1
274	-2.19	SNORD46
275	-2.22	SNORD91B
276	-2.23	MIR4729
277	-2.23	AQP7
278	-2.25	SNORD71
279	-2.26	MIR601
280	-2.27	MIR4506
281	-2.3	SCARNA5
282	-2.33	PRKXP1
283	-2.35	SNORD111
284	-2.35	SNORD116-24
285	-2.35	SNORA80A
286	-2.35	NPIPB11
287	-2.37	RNU6-79P
288	-2.37	SNORD60
289	-2.41	LOC105379251
290	-2.42	AMICA1
291	-2.42	SCARNA3
292	-2.43	SPRR2F
293	-2.44	MIR548AL
294	-2.44	TPT1
295	-2.44	SCARNA10
296	-2.46	SNORD17
297	-2.46	SNORA14A
298	-2.46	LOC100131541
299	-2.48	SNORA57; METTL12
300	-2.51	UBE2CP5
301	-2.54	SNORA71A
302	-2.58	LOC100506123
303	-2.58	SLAMF8
304	-2.59	SNORA2A
305	-2.62	TTN
306	-2.62	ABCG1
307	-2.63	TRAJ25
308	-2.64	TRAJ1
309	-2.64	RBMS3
310	-2.72	TRAJ19
311	-2.74	SNORA38B
312	-2.76	SLC14A1
313	-2.78	TRAJ14
314	-2.79	MPP7

315	-2.85	SNORA71D
316	-2.87	NUAK2
317	-2.96	SNORD15B
318	-2.98	SCARNA6
319	-2.99	PIK3IP1
320	-3	SNORA2C; MIR1291
321	-3.04	PLCG1
322	-3.04	SNORD3D
323	-3.18	SNORA54
324	-3.3	IGANRP
325	-3.32	NELL2
326	-3.5	SNORA60
327	-3.59	SNORA10; RPS2
328	-3.61	MIR1299
329	-3.68	MIR1203
330	-3.76	SNORA50C; SNHG25
331	-4.06	SNORA23

Supplemental Table 2. KEGG Analysis, day 14

#pathway ID	Pathway description	Observed gene count	False discovery rate	Matching proteins in your network
5321	Inflammatory bowel disease (IBD)	8	1.71E-10	HLA-DQA2,HLA-DRA,IL23R,IL4,IL4R,IL5,JUN,TNF
4060	Cytokine-cytokine receptor interaction	11	6.52E-10	CCL1,CCR7,IL23R,IL4,IL4R,IL5,TNF,TNFRSF1A,TNFRSF1B,TNFRSF4,TNFSF4
4380	Osteoclast differentiation	8	1.58E-08	FOS,FOSL2,JUN,JUNB,JUND,SOCS1,TNF,TNFRSF1A
5310	Asthma	5	2.20E-07	HLA-DQA2,HLA-DRA,IL4,IL5,TNF
5140	Leishmaniasis	6	3.74E-07	FOS,HLA-DQA2,HLA-DRA,IL4,JUN,TNF
5330	Allograft rejection	5	4.10E-07	HLA-DQA2,HLA-DRA,IL4,IL5,TNF
5164	Influenza A	7	2.11E-06	HLA-DQA2,HLA-DRA,HSPA6,JUN,TLR7,TNF,TNFRSF1A
4668	TNF signaling pathway	6	3.14E-06	FOS,JUN,JUNB,TNF,TNFRSF1A,TNFRSF1B
5145	Toxoplasmosis	6	3.88E-06	HLA-DQA2,HLA-DRA,HSPA6,SOCS1,TNF,TNFRSF1A
4640	Hematopoietic cell lineage	5	2.24E-05	HLA-DRA,IL4,IL4R,IL5,TNF
5166	HTLV-I infection	7	2.24E-05	EGR1,FOS,HLA-DQA2,HLA-DRA,JUN,TNF,TNFRSF1A
5323	Rheumatoid arthritis	5	2.24E-05	FOS,HLA-DQA2,HLA-DRA,JUN,TNF
5168	Herpes simplex infection	6	3.60E-05	FOS,HLA-DQA2,HLA-DRA,JUN,TNF,TNFRSF1A
4660	T cell receptor signaling pathway	5	3.89E-05	FOS,IL4,IL5,JUN,TNF
4672	Intestinal immune network for IgA production	4	4.13E-05	HLA-DQA2,HLA-DRA,IL4,IL5
5320	Autoimmune thyroid disease	4	6.00E-05	HLA-DQA2,HLA-DRA,IL4,IL5
5211	Renal cell carcinoma	4	0.000166	ARNT,EGLN3,EPAS1,JUN
4612	Antigen processing and presentation	4	0.000177	HLA-DQA2,HLA-DRA,HSPA6,TNF
4010	MAPK signaling pathway	6	0.000202	FOS,HSPA6,JUN,JUND,TNF,TNFRSF1A
4630	Jak-STAT signaling pathway	5	0.000248	IL23R,IL4,IL4R,IL5,SOCS1
5322	Systemic lupus erythematosus	4	0.000615	HLA-DQA2,HLA-DRA,SNRPD1,TNF
5142	Chagas disease (American trypanosomiasis)	4	0.000637	FOS,JUN,TNF,TNFRSF1A
5200	Pathways in cancer	6	0.000653	ARNT,EGLN3,EPAS1,FOS,JUN,RUNX1T1
4620	Toll-like receptor signaling pathway	4	0.000684	FOS,JUN,TLR7,TNF
5332	Graft-versus-host disease	3	0.000684	HLA-DQA2,HLA-DRA,TNF
4940	Type I diabetes mellitus	3	0.000894	HLA-DQA2,HLA-DRA,TNF
5014	Amyotrophic lateral sclerosis (ALS)	3	0.00168	TNF,TNFRSF1A,TNFRSF1B
4664	Fc epsilon RI signaling pathway	3	0.0037	IL4,IL5,TNF
4920	Adipocytokine signaling pathway	3	0.00373	TNF,TNFRSF1A,TNFRSF1B
5133	Pertussis	3	0.00394	FOS,JUN,TNF
5152	Tuberculosis	4	0.00408	HLA-DQA2,HLA-DRA,TNF,TNFRSF1A
5169	Epstein-Barr virus infection	4	0.00589	HLA-DQA2,HLA-DRA,HSPA6,JUN
4915	Estrogen signaling pathway	3	0.00856	FOS,HSPA6,JUN
3040	Spliceosome	3	0.019	HSPA6,SNRPD1,SNRPF
5162	Measles	3	0.0206	HSPA6,IL4,TLR7
5161	Hepatitis B	3	0.0248	FOS,JUN,TNF
4932	Non-alcoholic fatty liver disease (NAFLD)	3	0.0282	JUN,TNF,TNFRSF1A
4930	Type II diabetes mellitus	2	0.0305	SOCS1,TNF
5010	Alzheimer s disease	3	0.0354	BACE2,TNF,TNFRSF1A
5202	Transcriptional misregulation in cancer	3	0.0354	CCR7,NR4A3,RUNX1T1
5150	Staphylococcus aureus infection	2	0.0361	HLA-DQA2,HLA-DRA
5134	Legionellosis	2	0.038	HSPA6,TNF
5416	Viral myocarditis	2	0.0399	HLA-DQA2,HLA-DRA
5210	Colorectal cancer	2	0.0418	FOS,JUN

Supplemental Table 2. KEGG Analysis, day 21

#pathway ID	Pathway description	Observed gene count	False discovery rate	Matching proteins in your network
4060	Cytokine-cytokine receptor interaction	12	1.83E-08	CCL3,CRLF2,CSF2,IFNG,IL13,IL17RB,IL1A,IL3RA,IL4,IL5,OSM,TNFSF15
4630	Jak-STAT signaling pathway	8	6.99E-06	CRLF2,CSF2,IFNG,IL13,IL3RA,IL4,IL5,OSM
4110	Cell cycle	6	0.000192	CCNA1,CCNA2,CCNB1,CCNB2,CDC20,CDC45
4664	Fc epsilon RI signaling pathway	5	0.000192	CSF2,IL13,IL4,IL5,PLCG1
5321	Inflammatory bowel disease (IBD)	5	0.000192	IFNG,IL13,IL1A,IL4,IL5
5330	Allograft rejection	4	0.000244	CD86,IFNG,IL4,IL5
4640	Hematopoietic cell lineage	5	0.00036	CSF2,IL1A,IL3RA,IL4,IL5
5323	Rheumatoid arthritis	5	0.00036	CCL3,CD86,CSF2,IFNG,IL1A
4660	T cell receptor signaling pathway	5	0.00064	CSF2,IFNG,IL4,IL5,PLCG1
5162	Measles	5	0.00215	IFNG,IL13,IL1A,IL4,TP73
5140	Leishmaniasis	4	0.00227	IFNG,IL1A,IL4,PTGS2
5310	Asthma	3	0.00271	IL13,IL4,IL5
4914	Progesterone-mediated oocyte maturation	4	0.00325	CCNA1,CCNA2,CCNB1,CCNB2
5132	Salmonella infection	4	0.00332	CCL3,CSF2,IFNG,IL1A
5332	Graft-versus-host disease	3	0.00463	CD86,IFNG,IL1A
5322	Systemic lupus erythematosus	4	0.00516	CD86,HIST1H2AJ,HIST1H2BM,IFNG
4940	Type I diabetes mellitus	3	0.0056	CD86,IFNG,IL1A
4114	Oocyte meiosis	4	0.00665	CCNB1,CCNB2,CDC20,SGOL1
4672	Intestinal immune network for IgA production	3	0.00665	CD86,IL4,IL5
5320	Autoimmune thyroid disease	3	0.00869	CD86,IL4,IL5
4115	p53 signaling pathway	3	0.0197	CCNB1,CCNB2,TP73
5202	Transcriptional misregulation in cancer	4	0.03	CCNA1,CD86,CSF2,DUSP6
5203	Viral carcinogenesis	4	0.0409	CCNA1,CCNA2,CDC20,HIST1H2BM
5169	Epstein-Barr virus infection	4	0.0457	CCNA1,CCNA2,IFNG,PLCG1

Supplemental Table 3. Gene Ontogeny Analysis, day 14

#pathway ID	Pathway description	Observed gene count	False discovery rate
GO.0034097	response to cytokine	14	8.87E-08
GO.0051707	response to other organism	14	8.87E-08
GO.1903708	positive regulation of hemopoiesis	9	9.32E-08
GO.1902107	positive regulation of leukocyte differentiation	8	4.32E-07
GO.0033993	response to lipid	13	3.61E-06
GO.0032496	response to lipopolysaccharide	9	5.37E-06
GO.0002639	positive regulation of immunoglobulin production	5	5.66E-06
GO.0006954	inflammatory response	10	1.01E-05
GO.0031347	regulation of defense response	12	1.19E-05
GO.0009617	response to bacterium	10	1.44E-05
GO.0045639	positive regulation of myeloid cell differentiation	6	1.44E-05
GO.0051239	regulation of multicellular organismal process	19	1.44E-05
GO.0009893	positive regulation of metabolic process	22	3.44E-05
GO.0042127	regulation of cell proliferation	15	3.44E-05
GO.0019221	cytokine-mediated signaling pathway	9	3.62E-05
GO.0002763	positive regulation of myeloid leukocyte differentiation	5	5.25E-05
GO.0046636	negative regulation of alpha-beta T cell activation	4	5.25E-05
GO.0006955	immune response	14	5.39E-05
GO.0045637	regulation of myeloid cell differentiation	7	5.79E-05
GO.0002761	regulation of myeloid leukocyte differentiation	6	6.62E-05
GO.0046634	regulation of alpha-beta T cell activation	5	7.88E-05
GO.1903530	regulation of secretion by cell	10	9.38E-05
GO.1903706	regulation of hemopoiesis	8	9.38E-05
GO.0045622	regulation of T-helper cell differentiation	4	9.86E-05
GO.0031325	positive regulation of cellular metabolic process	19	0.000115
GO.0002376	immune system process	16	0.000143
GO.0071241	cellular response to inorganic substance	6	0.000143
GO.0070887	cellular response to chemical stimulus	17	0.000156
GO.1902105	regulation of leukocyte differentiation	7	0.000156
GO.0002699	positive regulation of immune effector process	6	0.00017
GO.0010534	regulation of activation of JAK2 kinase activity	3	0.000175
GO.0010604	positive regulation of macromolecule metabolic process	18	0.000185
GO.0001817	regulation of cytokine production	9	0.000211
GO.0045623	negative regulation of T-helper cell differentiation	3	0.000211
GO.0050727	regulation of inflammatory response	7	0.000211
GO.0051024	positive regulation of immunoglobulin secretion	3	0.000211
GO.0061418	regulation of transcription from RNA polymerase II promoter in response to hypoxia	4	0.000211
GO.0071345	cellular response to cytokine stimulus	9	0.000211
GO.0071310	cellular response to organic substance	15	0.000238
GO.0009605	response to external stimulus	15	0.00027
GO.0048518	positive regulation of biological process	24	0.000333
GO.0001774	microglial cell activation	3	0.000354
GO.0046425	regulation of JAK-STAT cascade	5	0.000354
GO.0010035	response to inorganic substance	8	0.000384
GO.0051716	cellular response to stimulus	26	0.000384
GO.0060341	regulation of cellular localization	12	0.000394
GO.0051591	response to cAMP	5	0.000436
GO.0071277	cellular response to calcium ion	4	0.000481
GO.0009612	response to mechanical stimulus	6	0.000595
GO.0051249	regulation of lymphocyte activation	7	0.000868
GO.0071248	cellular response to metal ion	5	0.000872
GO.2000525	positive regulation of T cell costimulation	2	0.000875
GO.0042510	regulation of tyrosine phosphorylation of Stat1 protein	3	0.00095
GO.0042110	T cell activation	6	0.000952
GO.0051251	positive regulation of lymphocyte activation	6	0.000952
GO.0032101	regulation of response to external stimulus	10	0.000968
GO.0030888	regulation of B cell proliferation	4	0.000981
GO.0001819	positive regulation of cytokine production	7	0.00105
GO.0051240	positive regulation of multicellular organismal process	12	0.00105
GO.0007165	signal transduction	22	0.00106
GO.0010557	positive regulation of macromolecule biosynthetic process	13	0.00106
GO.0043618	regulation of transcription from RNA polymerase II promoter in response to stress	4	0.00106
GO.0050707	regulation of cytokine secretion	5	0.00106
GO.0045624	positive regulation of T-helper cell differentiation	3	0.00113
GO.0048584	positive regulation of response to stimulus	14	0.00113
GO.0051090	regulation of sequence-specific DNA binding transcription factor activity	7	0.00113
GO.0051704	multi-organism process	15	0.00121

GO.0032103	positive regulation of response to external stimulus	7	0.00123
GO.0050708	regulation of protein secretion	7	0.0013
GO.0006952	defense response	12	0.00132
GO.0045935	positive regulation of nucleobase-containing compound metabolic process	13	0.00132
GO.0002825	regulation of T-helper 1 type immune response	3	0.00134
GO.0045893	positive regulation of transcription, DNA-templated	12	0.00134
GO.0048522	positive regulation of cellular process	21	0.00134
GO.0080134	regulation of response to stress	12	0.00134
GO.0045582	positive regulation of T cell differentiation	4	0.00142
GO.0046427	positive regulation of JAK-STAT cascade	4	0.00142
GO.0045321	leukocyte activation	7	0.00145
GO.0001562	response to protozoan	3	0.00147
GO.0002697	regulation of immune effector process	7	0.00152
GO.0031328	positive regulation of cellular biosynthetic process	13	0.00157
GO.0048534	hematopoietic or lymphoid organ development	8	0.00157
GO.0045626	negative regulation of T-helper 1 cell differentiation	2	0.00159
GO.0048583	regulation of response to stimulus	18	0.0017
GO.0042104	positive regulation of activated T cell proliferation	3	0.00175
GO.0002520	immune system development	8	0.00193
GO.0007166	cell surface receptor signaling pathway	14	0.00193
GO.0042493	response to drug	7	0.00193
GO.0044700	single organism signaling	22	0.00203
GO.0014070	response to organic cyclic compound	9	0.00207
GO.0008284	positive regulation of cell proliferation	9	0.00209
GO.0042325	regulation of phosphorylation	11	0.00216
GO.0045597	positive regulation of cell differentiation	9	0.00216
GO.0002521	leukocyte differentiation	6	0.0022
GO.0006950	response to stress	18	0.0022
GO.0051246	regulation of protein metabolic process	15	0.00234
GO.0002684	positive regulation of immune system process	9	0.00236
GO.0050670	regulation of lymphocyte proliferation	5	0.0025
GO.0032649	regulation of interferon-gamma production	4	0.00253
GO.0048295	positive regulation of isotype switching to IgE isotypes	2	0.00253
GO.0048519	negative regulation of biological process	20	0.00253
GO.1903532	positive regulation of secretion by cell	6	0.00253
GO.2000416	regulation of eosinophil migration	2	0.00253
GO.0007154	cell communication	22	0.00254
GO.0010033	response to organic substance	15	0.00259
GO.0010647	positive regulation of cell communication	12	0.0026
GO.0002823	negative regulation of adaptive immune response based on somatic recombination of immune rece	3	0.00274
GO.0031399	regulation of protein modification process	12	0.00274
GO.0032735	positive regulation of interleukin-12 production	3	0.00274
GO.0043304	regulation of mast cell degranulation	3	0.00274
GO.0050729	positive regulation of inflammatory response	4	0.00282
GO.0002698	negative regulation of immune effector process	4	0.00305
GO.0002682	regulation of immune system process	11	0.0032
GO.0001892	embryonic placenta development	4	0.00326
GO.0051094	positive regulation of developmental process	10	0.00326
GO.0033209	tumor necrosis factor-mediated signaling pathway	3	0.0035
GO.0050728	negative regulation of inflammatory response	4	0.0035
GO.0051247	positive regulation of protein metabolic process	11	0.00391
GO.0030099	myeloid cell differentiation	5	0.00399
GO.0032268	regulation of cellular protein metabolic process	14	0.004
GO.0050864	regulation of B cell activation	4	0.00442
GO.0006979	response to oxidative stress	6	0.00463
GO.0030890	positive regulation of B cell proliferation	3	0.00464
GO.0032653	regulation of interleukin-10 production	3	0.00464
GO.0030097	hemopoiesis	7	0.00474
GO.0001932	regulation of protein phosphorylation	10	0.00483
GO.0043382	positive regulation of memory T cell differentiation	2	0.00483
GO.0051133	regulation of NK T cell activation	2	0.00483
GO.2000319	regulation of T-helper 17 cell differentiation	2	0.00483
GO.0050730	regulation of peptidyl-tyrosine phosphorylation	5	0.00484
GO.0098542	defense response to other organism	6	0.00492
GO.0050671	positive regulation of lymphocyte proliferation	4	0.00493
GO.0051049	regulation of transport	12	0.005
GO.0051223	regulation of protein transport	8	0.00543
GO.0050777	negative regulation of immune response	4	0.00559
GO.0001816	cytokine production	4	0.00609
GO.0032870	cellular response to hormone stimulus	7	0.00613

GO.0031349	positive regulation of defense response	6	0.0062
GO.0032722	positive regulation of chemokine production	3	0.00647
GO.0071456	cellular response to hypoxia	4	0.0065
GO.0045944	positive regulation of transcription from RNA polymerase II promoter	9	0.00722
GO.0030217	T cell differentiation	4	0.00768
GO.0043619	regulation of transcription from RNA polymerase II promoter in response to oxidative stress	2	0.00776
GO.0045630	positive regulation of T-helper 2 cell differentiation	2	0.00776
GO.2000113	negative regulation of cellular macromolecule biosynthetic process	10	0.00799
GO.0050776	regulation of immune response	8	0.00887
GO.0048545	response to steroid hormone	6	0.00889
GO.0010646	regulation of cell communication	15	0.00901
GO.0048585	negative regulation of response to stimulus	10	0.00952
GO.0045934	negative regulation of nucleobase-containing compound metabolic process	10	0.00972
GO.1901654	response to ketone	4	0.00997
GO.0046631	alpha-beta T cell activation	3	0.0102
GO.0010605	negative regulation of macromolecule metabolic process	13	0.0104
GO.0002703	regulation of leukocyte mediated immunity	4	0.0109
GO.0031324	negative regulation of cellular metabolic process	13	0.011
GO.0032729	positive regulation of interferon-gamma production	3	0.0111
GO.0042531	positive regulation of tyrosine phosphorylation of STAT protein	3	0.0111
GO.0032736	positive regulation of interleukin-13 production	2	0.0113
GO.0035914	skeletal muscle cell differentiation	3	0.0115
GO.0048568	embryonic organ development	6	0.0128
GO.0001890	placenta development	4	0.0131
GO.0009628	response to abiotic stimulus	9	0.0133
GO.0045892	negative regulation of transcription, DNA-templated	9	0.0142
GO.0002824	positive regulation of adaptive immune response based on somatic recombination of immune rece	3	0.0151
GO.0017157	regulation of exocytosis	4	0.0151
GO.0045670	regulation of osteoclast differentiation	3	0.0151
GO.0030854	positive regulation of granulocyte differentiation	2	0.0153
GO.0050871	positive regulation of B cell activation	3	0.0154
GO.0071496	cellular response to external stimulus	5	0.0154
GO.0050731	positive regulation of peptidyl-tyrosine phosphorylation	4	0.0155
GO.0002708	positive regulation of lymphocyte mediated immunity	3	0.016
GO.0023056	positive regulation of signaling	10	0.0172
GO.0009966	regulation of signal transduction	13	0.0187
GO.0045595	regulation of cell differentiation	10	0.0196
GO.0043306	positive regulation of mast cell degranulation	2	0.0199
GO.0045921	positive regulation of exocytosis	3	0.0202
GO.0034162	toll-like receptor 9 signaling pathway	3	0.0224
GO.0046649	lymphocyte activation	5	0.0224
GO.0048523	negative regulation of cellular process	17	0.0224
GO.0071260	cellular response to mechanical stimulus	3	0.0224
GO.0000302	response to reactive oxygen species	4	0.0225
GO.0008630	intrinsic apoptotic signaling pathway in response to DNA damage	3	0.0232
GO.0051241	negative regulation of multicellular organismal process	8	0.0239
GO.0071560	cellular response to transforming growth factor beta stimulus	4	0.0243
GO.0050714	positive regulation of protein secretion	4	0.0247
GO.2000026	regulation of multicellular organismal development	10	0.0254
GO.0001829	trophectodermal cell differentiation	2	0.0274
GO.0002705	positive regulation of leukocyte mediated immunity	3	0.0274
GO.0042523	positive regulation of tyrosine phosphorylation of Stat5 protein	2	0.0274
GO.0097190	apoptotic signaling pathway	5	0.0274
GO.1901741	positive regulation of myoblast fusion	2	0.0274
GO.0043523	regulation of neuron apoptotic process	4	0.0282
GO.0002755	MyD88-dependent toll-like receptor signaling pathway	3	0.0299
GO.0048145	regulation of fibroblast proliferation	3	0.0299
GO.0033233	regulation of protein sumoylation	2	0.03
GO.0042832	defense response to protozoan	2	0.03
GO.1902106	negative regulation of leukocyte differentiation	3	0.0305
GO.0032270	positive regulation of cellular protein metabolic process	9	0.0318
GO.0050778	positive regulation of immune response	6	0.0324
GO.0009967	positive regulation of signal transduction	9	0.0325
GO.0002076	osteoblast development	2	0.0328
GO.0035994	response to muscle stretch	2	0.0328
GO.0019222	regulation of metabolic process	22	0.036
GO.0033554	cellular response to stress	10	0.0374
GO.0032660	regulation of interleukin-17 production	2	0.0392
GO.0042326	negative regulation of phosphorylation	5	0.0398
GO.0002293	alpha-beta T cell differentiation involved in immune response	2	0.0421

GO.0045672	positive regulation of osteoclast differentiation	2	0.0421
GO.0071356	cellular response to tumor necrosis factor	3	0.0425
GO.0002573	myeloid leukocyte differentiation	3	0.0433
GO.0006357	regulation of transcription from RNA polymerase II promoter	10	0.0433
GO.0007178	transmembrane receptor protein serine/threonine kinase signaling pathway	4	0.0433
GO.0032733	positive regulation of interleukin-10 production	2	0.0444
GO.0065009	regulation of molecular function	13	0.0444
GO.0071624	positive regulation of granulocyte chemotaxis	2	0.0444
GO.0044708	single-organism behavior	5	0.0451
GO.0031327	negative regulation of cellular biosynthetic process	9	0.0476
GO.0034695	response to prostaglandin E	2	0.0476
GO.0043030	regulation of macrophage activation	2	0.0476
GO.0031323	regulation of cellular metabolic process	20	0.0485

Supplemental Table 3. Gene Ontogeny Analysis, day 21

#pathway ID	Pathway description	Observed gene count	False discovery rate
GO.0000278	mitotic cell cycle	67	2.00E-34
GO.1903047	mitotic cell cycle process	57	1.46E-27
GO.0007049	cell cycle	72	7.91E-27
GO.0022402	cell cycle process	62	1.12E-24
GO.0007067	mitotic nuclear division	39	6.56E-24
GO.0051301	cell division	42	8.18E-22
GO.0000280	nuclear division	40	1.50E-21
GO.0048285	organelle fission	41	1.50E-21
GO.0007059	chromosome segregation	27	1.62E-18
GO.0051726	regulation of cell cycle	45	2.17E-13
GO.0000070	mitotic sister chromatid segregation	16	2.97E-13
GO.0010564	regulation of cell cycle process	34	3.07E-13
GO.0044772	mitotic cell cycle phase transition	27	6.28E-13
GO.0098813	nuclear chromosome segregation	18	3.39E-12
GO.0006259	DNA metabolic process	36	1.81E-11
GO.0051983	regulation of chromosome segregation	14	2.19E-11
GO.0006260	DNA replication	21	2.64E-11
GO.0071103	DNA conformation change	21	5.04E-11
GO.0006996	organelle organization	75	1.07E-10
GO.1902589	single-organism organelle organization	60	1.38E-10
GO.0000083	regulation of transcription involved in G1/S transition of mitot	10	1.54E-10
GO.1901990	regulation of mitotic cell cycle phase transition	21	1.11E-09
GO.0051302	regulation of cell division	21	1.71E-09
GO.0006323	DNA packaging	17	1.86E-09
GO.0051276	chromosome organization	37	1.86E-09
GO.0000075	cell cycle checkpoint	19	8.42E-09
GO.0007346	regulation of mitotic cell cycle	26	1.09E-08
GO.0000082	G1/S transition of mitotic cell cycle	17	1.13E-08
GO.0006261	DNA-dependent DNA replication	13	1.13E-08
GO.0007264	small GTPase mediated signal transduction	31	1.14E-08
GO.0051716	cellular response to stimulus	111	2.23E-08
GO.0035556	intracellular signal transduction	53	2.27E-08
GO.0044763	single-organism cellular process	156	7.38E-08
GO.0007088	regulation of mitotic nuclear division	14	8.91E-08
GO.0016043	cellular component organization	94	9.74E-08
GO.0051783	regulation of nuclear division	15	9.74E-08
GO.0045787	positive regulation of cell cycle	20	2.15E-07
GO.0090068	positive regulation of cell cycle process	18	2.40E-07
GO.0006270	DNA replication initiation	8	2.43E-07
GO.0045931	positive regulation of mitotic cell cycle	13	2.62E-07
GO.0010948	negative regulation of cell cycle process	17	8.17E-07
GO.0051781	positive regulation of cell division	13	1.33E-06
GO.0006281	DNA repair	22	1.35E-06
GO.0006334	nucleosome assembly	12	1.75E-06
GO.0065004	protein-DNA complex assembly	13	1.83E-06
GO.0051782	negative regulation of cell division	10	3.24E-06
GO.1901992	positive regulation of mitotic cell cycle phase transition	9	3.61E-06
GO.0000727	double-strand break repair via break-induced replication	4	5.49E-06
GO.0031497	chromatin assembly	12	5.84E-06

GO.0050789	regulation of biological process	142	9.56E-06
GO.0007052	mitotic spindle organization	8	1.01E-05
GO.0000910	cytokinesis	10	1.20E-05
GO.0045786	negative regulation of cell cycle	21	1.36E-05
GO.0002376	immune system process	49	1.37E-05
GO.0030071	regulation of mitotic metaphase/anaphase transition	8	1.37E-05
GO.0044699	single-organism process	153	2.06E-05
GO.0050794	regulation of cellular process	137	2.06E-05
GO.0006461	protein complex assembly	31	2.45E-05
GO.0070271	protein complex biogenesis	31	2.45E-05
GO.0000086	G2/M transition of mitotic cell cycle	12	2.76E-05
GO.0022616	DNA strand elongation	7	2.76E-05
GO.0071822	protein complex subunit organization	39	2.98E-05
GO.0006336	DNA replication-independent nucleosome assembly	8	4.24E-05
GO.0034622	cellular macromolecular complex assembly	23	5.51E-05
GO.0000226	microtubule cytoskeleton organization	17	5.66E-05
GO.0042127	regulation of cell proliferation	39	5.86E-05
GO.1902850	microtubule cytoskeleton organization involved in mitosis	6	5.86E-05
GO.0001932	regulation of protein phosphorylation	34	6.07E-05
GO.0006950	response to stress	68	6.07E-05
GO.0031577	spindle checkpoint	7	6.57E-05
GO.0051784	negative regulation of nuclear division	8	6.85E-05
GO.0000076	DNA replication checkpoint	5	7.56E-05
GO.0006955	immune response	36	7.94E-05
GO.0042325	regulation of phosphorylation	35	9.93E-05
GO.0007051	spindle organization	9	0.000101
GO.0010965	regulation of mitotic sister chromatid separation	7	0.000101
GO.0023052	signaling	87	0.000101
GO.0034080	CENP-A containing nucleosome assembly	7	0.000101
GO.0061641	CENP-A containing chromatin organization	7	0.000101
GO.0051984	positive regulation of chromosome segregation	5	0.000103
GO.0065007	biological regulation	141	0.00012
GO.0007017	microtubule-based process	20	0.000122
GO.0032434	regulation of proteasomal ubiquitin-dependent protein catab	11	0.000122
GO.0045840	positive regulation of mitotic nuclear division	7	0.000128
GO.1990267	response to transition metal nanoparticle	10	0.000128
GO.0006974	cellular response to DNA damage stimulus	24	0.000153
GO.0044700	single organism signaling	86	0.000167
GO.0048523	negative regulation of cellular process	73	0.000167
GO.0051303	establishment of chromosome localization	7	0.000167
GO.0007165	signal transduction	82	0.000173
GO.0048519	negative regulation of biological process	77	0.000173
GO.0051128	regulation of cellular component organization	48	0.000201
GO.0002274	myeloid leukocyte activation	9	0.000204
GO.0051246	regulation of protein metabolic process	52	0.000214
GO.0042493	response to drug	18	0.000222
GO.0010389	regulation of G2/M transition of mitotic cell cycle	7	0.000242
GO.0006271	DNA strand elongation involved in DNA replication	6	0.000254
GO.0000003	reproduction	28	0.000266
GO.0045930	negative regulation of mitotic cell cycle	13	0.0003
GO.0050896	response to stimulus	108	0.000313
GO.0065003	macromolecular complex assembly	32	0.000313

GO.1901991	negative regulation of mitotic cell cycle phase transition	11	0.000356
GO.0006310	DNA recombination	12	0.000358
GO.0034097	response to cytokine	22	0.000358
GO.0007154	cell communication	86	0.000361
GO.0090307	mitotic spindle assembly	5	0.000374
GO.0060326	cell chemotaxis	11	0.000388
GO.0061640	cytoskeleton-dependent cytokinesis	6	0.000395
GO.0009636	response to toxic substance	11	0.000406
GO.0006302	double-strand break repair	10	0.000492
GO.0007093	mitotic cell cycle checkpoint	11	0.000501
GO.0016477	cell migration	24	0.000501
GO.0097305	response to alcohol	15	0.000501
GO.0051985	negative regulation of chromosome segregation	6	0.00053
GO.0008285	negative regulation of cell proliferation	22	0.00055
GO.0031399	regulation of protein modification process	38	0.00055
GO.0034341	response to interferon-gamma	9	0.00055
GO.0033044	regulation of chromosome organization	12	0.000574
GO.0002449	lymphocyte mediated immunity	9	0.000578
GO.0007010	cytoskeleton organization	25	0.000581
GO.0006952	defense response	35	0.000592
GO.0031145	anaphase-promoting complex-dependent proteasomal ubiqui	8	0.000607
GO.0051988	regulation of attachment of spindle microtubules to kinetocho	4	0.000628
GO.1903050	regulation of proteolysis involved in cellular protein catabolic	14	0.00072
GO.0051338	regulation of transferase activity	26	0.000758
GO.0002443	leukocyte mediated immunity	10	0.000829
GO.0051297	centrosome organization	7	0.000829
GO.0007076	mitotic chromosome condensation	4	0.000901
GO.0019220	regulation of phosphate metabolic process	36	0.000987
GO.0030261	chromosome condensation	5	0.001
GO.0032465	regulation of cytokinesis	7	0.001
GO.0006928	movement of cell or subcellular component	33	0.00101
GO.0009411	response to UV	9	0.00101
GO.0051321	meiotic cell cycle	10	0.00114
GO.0008608	attachment of spindle microtubules to kinetochore	4	0.00119
GO.0031570	DNA integrity checkpoint	10	0.00119
GO.0046427	positive regulation of JAK-STAT cascade	7	0.00119
GO.0061136	regulation of proteasomal protein catabolic process	12	0.00119
GO.0032268	regulation of cellular protein metabolic process	47	0.00131
GO.0000281	mitotic cytokinesis	5	0.00138
GO.0010165	response to X-ray	5	0.00138
GO.0050731	positive regulation of peptidyl-tyrosine phosphorylation	10	0.00143
GO.0030162	regulation of proteolysis	23	0.00146
GO.0034508	centromere complex assembly	6	0.00153
GO.0045839	negative regulation of mitotic nuclear division	6	0.00153
GO.0007096	regulation of exit from mitosis	4	0.00155
GO.0043306	positive regulation of mast cell degranulation	4	0.00155
GO.0051674	localization of cell	24	0.00159
GO.0032776	DNA methylation on cytosine	5	0.00187
GO.0040011	locomotion	30	0.00194
GO.1902531	regulation of intracellular signal transduction	33	0.00217
GO.0000724	double-strand break repair via homologous recombination	7	0.00226
GO.0010212	response to ionizing radiation	9	0.00232

GO.1903557	positive regulation of tumor necrosis factor superfamily cytok	6	0.00233
GO.0051247	positive regulation of protein metabolic process	33	0.00237
GO.0006954	inflammatory response	16	0.00252
GO.0042176	regulation of protein catabolic process	16	0.00252
GO.0031536	positive regulation of exit from mitosis	3	0.00254
GO.0022607	cellular component assembly	39	0.00261
GO.0002252	immune effector process	16	0.00278
GO.0031572	G2 DNA damage checkpoint	5	0.00281
GO.0034502	protein localization to chromosome	5	0.00281
GO.0001934	positive regulation of protein phosphorylation	23	0.00285
GO.0033043	regulation of organelle organization	28	0.00296
GO.0042531	positive regulation of tyrosine phosphorylation of STAT protei	6	0.00304
GO.0007094	mitotic spindle assembly checkpoint	5	0.00322
GO.0032270	positive regulation of cellular protein metabolic process	31	0.00346
GO.0033554	cellular response to stress	36	0.0038
GO.0043933	macromolecular complex subunit organization	43	0.00389
GO.0044818	mitotic G2/M transition checkpoint	4	0.00389
GO.0032467	positive regulation of cytokinesis	5	0.00404
GO.0032435	negative regulation of proteasomal ubiquitin-dependent prote	6	0.00429
GO.0051310	metaphase plate congression	5	0.00458
GO.0070507	regulation of microtubule cytoskeleton organization	8	0.00466
GO.0051129	negative regulation of cellular component organization	18	0.00486
GO.0000079	regulation of cyclin-dependent protein serine/threonine kinas	7	0.00574
GO.0000183	chromatin silencing at rDNA	5	0.00574
GO.0002366	leukocyte activation involved in immune response	8	0.00574
GO.0006275	regulation of DNA replication	8	0.00574
GO.0060968	regulation of gene silencing	5	0.00574
GO.0043549	regulation of kinase activity	21	0.00584
GO.0045080	positive regulation of chemokine biosynthetic process	3	0.00585
GO.0051488	activation of anaphase-promoting complex activity	3	0.00585
GO.0071346	cellular response to interferon-gamma	7	0.00597
GO.0045732	positive regulation of protein catabolic process	11	0.00634
GO.1903052	positive regulation of proteolysis involved in cellular protein c	9	0.00649
GO.0051439	regulation of ubiquitin-protein ligase activity involved in mitot	7	0.00673
GO.0051656	establishment of organelle localization	12	0.00673
GO.0060333	interferon-gamma-mediated signaling pathway	6	0.0068
GO.0031401	positive regulation of protein modification process	26	0.00683
GO.0071345	cellular response to cytokine stimulus	17	0.00688
GO.0010035	response to inorganic substance	15	0.00697
GO.0051052	regulation of DNA metabolic process	12	0.0073
GO.0010639	negative regulation of organelle organization	12	0.00799
GO.0019221	cytokine-mediated signaling pathway	14	0.00802
GO.0045842	positive regulation of mitotic metaphase/anaphase transition	3	0.00802
GO.0045087	innate immune response	24	0.00814
GO.0042981	regulation of apoptotic process	31	0.0082
GO.1903660	negative regulation of complement-dependent cytotoxicity	2	0.00821
GO.0030593	neutrophil chemotaxis	5	0.00828
GO.0060341	regulation of cellular localization	28	0.00851
GO.1902533	positive regulation of intracellular signal transduction	22	0.00851
GO.0080090	regulation of primary metabolic process	83	0.00996
GO.0010941	regulation of cell death	32	0.0111
GO.0002228	natural killer cell mediated immunity	4	0.0115

GO.0033260	nuclear DNA replication	4	0.0115
GO.0045937	positive regulation of phosphate metabolic process	24	0.0115
GO.0044085	cellular component biogenesis	39	0.0121
GO.0033993	response to lipid	21	0.0122
GO.0051640	organelle localization	13	0.0122
GO.0065008	regulation of biological quality	53	0.0124
GO.1904029	regulation of cyclin-dependent protein kinase activity	8	0.0133
GO.0045862	positive regulation of proteolysis	13	0.0135
GO.0001774	microglial cell activation	3	0.0137
GO.0071168	protein localization to chromatin	3	0.0137
GO.0009314	response to radiation	15	0.014
GO.0032880	regulation of protein localization	23	0.014
GO.0014070	response to organic cyclic compound	21	0.0141
GO.0032760	positive regulation of tumor necrosis factor production	5	0.0141
GO.0045428	regulation of nitric oxide biosynthetic process	5	0.0141
GO.0008284	positive regulation of cell proliferation	21	0.0146
GO.0042116	macrophage activation	4	0.0146
GO.0046688	response to copper ion	4	0.0146
GO.0045859	regulation of protein kinase activity	19	0.0147
GO.0040008	regulation of growth	18	0.0152
GO.0042060	wound healing	19	0.0155
GO.0051179	localization	69	0.0158
GO.0010332	response to gamma radiation	5	0.0164
GO.0001701	in utero embryonic development	13	0.0176
GO.0002639	positive regulation of immunoglobulin production	4	0.0186
GO.0007080	mitotic metaphase plate congression	4	0.0186
GO.0009605	response to external stimulus	37	0.0186
GO.0048660	regulation of smooth muscle cell proliferation	6	0.0199
GO.0007275	multicellular organismal development	66	0.0202
GO.0034421	post-translational protein acetylation	2	0.0202
GO.1902947	regulation of tau-protein kinase activity	2	0.0202
GO.1902969	mitotic DNA replication	2	0.0202
GO.1902996	regulation of neurofibrillary tangle assembly	2	0.0202
GO.0007596	blood coagulation	16	0.0215
GO.0050900	leukocyte migration	10	0.0222
GO.1901214	regulation of neuron death	10	0.0222
GO.0045471	response to ethanol	7	0.023
GO.0002286	T cell activation involved in immune response	5	0.0238
GO.0001833	inner cell mass cell proliferation	3	0.0257
GO.0006978	DNA damage response, signal transduction by p53 class media	3	0.0257
GO.0032642	regulation of chemokine production	5	0.0257
GO.0002700	regulation of production of molecular mediator of immune re	6	0.0258
GO.2000060	positive regulation of protein ubiquitination involved in ubiqu	6	0.0258
GO.0010038	response to metal ion	11	0.0261
GO.0045321	leukocyte activation	13	0.0263
GO.0002285	lymphocyte activation involved in immune response	6	0.027
GO.0002702	positive regulation of production of molecular mediator of im	5	0.027
GO.0006968	cellular defense response	5	0.027
GO.0043065	positive regulation of apoptotic process	16	0.027
GO.0050729	positive regulation of inflammatory response	6	0.027
GO.0070887	cellular response to chemical stimulus	42	0.027
GO.1902532	negative regulation of intracellular signal transduction	13	0.027

GO.0090329	regulation of DNA-dependent DNA replication	4	0.0277
GO.1902229	regulation of intrinsic apoptotic signaling pathway in response	4	0.0277
GO.0010605	negative regulation of macromolecule metabolic process	41	0.0284
GO.0032501	multicellular organismal process	84	0.0284
GO.0051707	response to other organism	18	0.0284
GO.1903827	regulation of cellular protein localization	15	0.0285
GO.1903532	positive regulation of secretion by cell	11	0.0286
GO.0009991	response to extracellular stimulus	14	0.0299
GO.0044702	single organism reproductive process	24	0.0313
GO.0006468	protein phosphorylation	20	0.0314
GO.0031324	negative regulation of cellular metabolic process	41	0.0321
GO.2001252	positive regulation of chromosome organization	6	0.0324
GO.0044707	single-multicellular organism process	81	0.0327
GO.0045429	positive regulation of nitric oxide biosynthetic process	4	0.0329
GO.0051340	regulation of ligase activity	7	0.0335
GO.0001819	positive regulation of cytokine production	12	0.0343
GO.0043146	spindle stabilization	2	0.0343
GO.0006935	chemotaxis	17	0.0344
GO.0007141	male meiosis I	3	0.0344
GO.0042510	regulation of tyrosine phosphorylation of Stat1 protein	3	0.0344
GO.2001251	negative regulation of chromosome organization	6	0.0348
GO.0009987	cellular process	155	0.035
GO.0045143	homologous chromosome segregation	4	0.0355
GO.1901216	positive regulation of neuron death	5	0.0356
GO.0031323	regulation of cellular metabolic process	82	0.0381
GO.0032570	response to progesterone	4	0.0386
GO.0060255	regulation of macromolecule metabolic process	79	0.0391
GO.1903036	positive regulation of response to wounding	7	0.0398
GO.0009607	response to biotic stimulus	18	0.041
GO.0051054	positive regulation of DNA metabolic process	7	0.0414
GO.0010498	proteasomal protein catabolic process	11	0.0427
GO.0007127	meiosis I	5	0.0428
GO.0071241	cellular response to inorganic substance	7	0.0428
GO.2001020	regulation of response to DNA damage stimulus	7	0.0428
GO.0031667	response to nutrient levels	13	0.0436
GO.0051704	multi-organism process	40	0.0436
GO.0001556	oocyte maturation	3	0.0459
GO.0042832	defense response to protozoan	3	0.0459
GO.0009967	positive regulation of signal transduction	27	0.05
GO.0018105	peptidyl-serine phosphorylation	6	0.05
GO.0043066	negative regulation of apoptotic process	20	0.05